

The eruptive history of Turrialba volcano, Costa Rica, and potential hazards from future eruptions

Mark Reagan

Department of Geoscience, University of Iowa, Iowa City, Iowa 52242, USA

Eliecer Duarte

Observatorio Vulcanológico y Sismológico de Costa Rica (OVSICORI), Universidad Nacional, Apdo. 2346-3000, Heredia, Costa Rica

Gerardo J. Soto

Apdo. 360-2350, San Francisco 2 Ríos, Costa Rica

Erick Fernández

Observatorio Vulcanológico y Sismológico de Costa Rica (OVSICORI), Universidad Nacional, Apdo. 2346-3000, Heredia, Costa Rica

ABSTRACT

Turrialba volcano's high summit elevation and steep slopes, its position upwind of the Central Valley, and its record of explosive eruptions all suggest that it poses a significant threat to Costa Rican population and economy. To better understand the nature and significance of this threat, the geology, stratigraphy, and recent eruptive history of Turrialba were investigated. Outcrops of lava and pyroclastic units from at least 20 eruptions of basalt to dacite are recorded in Turrialba's summit area. The majority of these eruptions preceded a major erosional period that may have involved glaciation and that produced a prominent northeast-facing valley at Turrialba. This period also was apparently marked by a dearth of volcanism. The post-erosional period began with eruptions of massive andesite to dacite lava flows ca. 9300 yr B.P. Five of the six most recent eruptions, including the eruption of 1864–1866 A.D., were small volume (<0.03 km³) phreatic and phreatomagmatic explosive eruptions involving basalt and basaltic andesite. The exception was a Plinian eruption of silicic andesite at ca. 1970 yr B.P. with a volume of ~0.2 km³. Turrialba's next eruption will likely be similar to the recent eruptions of basaltic to basaltic andesitic composition, although a larger volume and more destructive eruption of silicic andesite to dacite also is possible.

Keywords: Costa Rica, volcanism, tephrostratigraphy, volcanic risk, glacial erosion, Turrialba.

INTRODUCTION

Turrialba, the southeasternmost young volcano in Costa Rica (Fig. 1), is Central America's second tallest volcano after nearby Irazú. These volcanoes are ~10 km apart and their combined volumes comprise the largest stratovolcano complex in Central America (Carr et al., 1990). Turrialba is upwind of the Central Valley of Costa Rica, which includes San José and most of Costa Rica's other large population centers, as well as its main international airport. Therefore, an eruption of Turrialba could pose a severe hazard to the economy of Costa Rica. Moreover, the frequent rainfall, dense radial hydrographic network, relatively sparse vegetation coverage on its upper flanks, and limited official measures for local emergency response suggest that an eruption of Turrialba could pose a particularly serious threat to its local population (Duarte, 1990).

Turrialba last erupted between 1864 and 1866, producing ash fallout deposits that extended into the Central Valley and a few pyroclastic surges that affected the summit of Turrialba. Lahars associated with this eruption flowed down river drainages, extending into towns surrounding the volcano. More recently, periodic seismic swarms and enhanced fumarolic activity have been observed at Turrialba since 1998 (Barboza et al., 2000; Fernández et al., 2002; Barboza et al., 2003; Mora et al., 2004). With this record of historical eruptions and recent activity, there is a strong likelihood that Turrialba will erupt explosively again.

This paper discusses the geology and tephra stratigraphy of the Turrialba summit region. It covers all of the geological units exposed in and near Turrialba's summit crater complex, but emphasizes units erupted in the past ~3400 yr because of their

better representation in the rock record. The reconstructed history is based on geological and stratigraphic observations, geochemical correlations between lavas and tephra (see Appendix Table A1), and radiocarbon ages (Table 1). The paper concludes with an assessment of the hazards posed by Turrialba volcano to its surrounding area.

TURRIALBA'S VOLCANIC HISTORY

The Turrialba massif overlies the complexly deformed Tertiary sediments of the Limón Basin, which are capped by andesite lavas dated at 2.15 ± 0.30 Ma (Tournon 1984; Soto, 1988). The edifice that was built during the current phase of volcanism at Turrialba overlies deeply eroded older volcanoes that in combination represent ~1 m.y. of arc-related volcanic activity (Bellon and Tournon, 1978; Gans et al., 2003). The currently active edifice has an elliptical crater that faces to the northeast and contains three interior craters labeled w (west), c (central), and e (east) based on their geographic position, as well as three exterior peaks: Cerro San Carlos to the north, Cerro San Enrique to the east, and Cerro San Juan to the southwest (Fig. 2). Normal faults cut through the summit region from near Cerro San Enrique to the southwest for several kilometers. Two pyroclastic cones named Tiendilla and El Armado, which are generally aligned with these northeast structural trends, lie 2–3 km southwest of Cerro San Juan and Cerro San Enrique (Soto, 1988).

At least 20 eruptions are recorded in the crater region of Turrialba, some of which are associated with major lava flows exposed along Turrialba's northern, western, and southern flanks (see Soto, 1988). The volcanic units associated with these eruptions are separated into two groups based on their stratigraphic relationship to a significant erosional period that may have been associated with glaciation (see below). The minimum age for the oldest volcanism recorded in the summit region is 9300 yr B.P., based on the age of the oldest post-erosional lavas. The maximum age is poorly constrained, but may be ca. 170,000 yr B.P. based on ^{40}Ar - ^{39}Ar dating of Central Valley volcanics (Gans et al., 2003). The oldest pre-erosional stratigraphic units cropping out in the crater region are medium- to high-K calcalkaline basalts, andesites, and dacites (see Table A1) that were vented by at least nine eruptions (units 15 and 14; Figs. 3 and 4). Lava flows and breccias of basaltic andesite (unit 13, 55 wt% SiO_2) and dacite (unit 12, 64 wt% SiO_2) that crop out along the northwest wall of crater c (Fig. 3) and the overlying andesitic 55–57 wt% SiO_2 pyroclastic breccias of unit 11 progressively overlie the lowermost units. These breccias, which also crop out in crater w and the southeast wall of crater c, likely represent several eruptions. Lake bed deposits consisting of finely bedded white to light gray clay and altered talus are exposed in the wall separating craters w and c, postdate unit 14 (Fig. 5), and predate the excavation and collapse that resulted in the modern crater complex. Medium-K calcalkaline basaltic andesite lavas (54–55 wt% SiO_2 ; see Table A1) that dip inward toward the center of crater w are designated as unit 10 (Fig. 6).

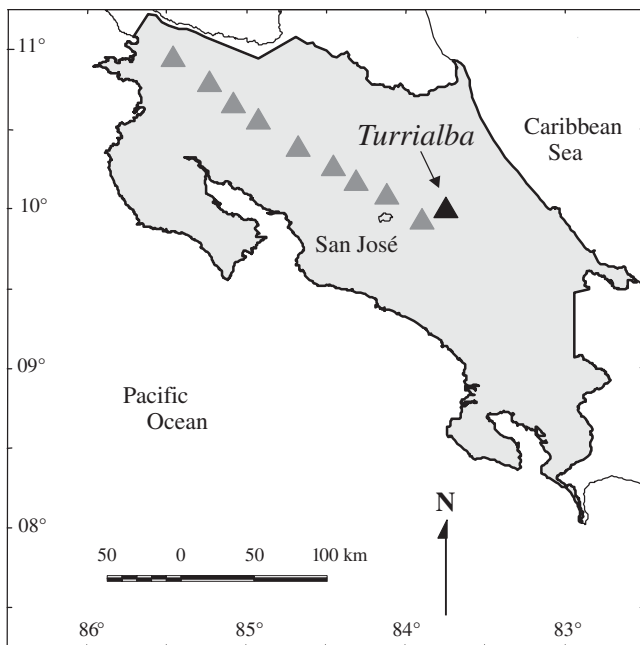


Figure 1. Location map for Turrialba volcano in Costa Rica.

TABLE 1. RADIOMETRIC AGES FOR SAMPLES FROM TURRIALBA VOLCANO

Sample	Unit	Material	Radiocarbon age (yr B.P.)	Calibrated calendar year ages [§]
89-3*	3	10 cm diameter peat log in phreatic explosion debris	1415 ± 75	644 A.D. (597–668 A.D.)
T-20-m-4	4	<1 cm charcoal fragments in pyroclastic flow (pf)	1860 ± 100	131 A.D. (31–318 A.D.)
T-100 [†]	4	3 cm diameter charcoal branch in fallout deposit	1975 ± 45	27–49 A.D. (38 B.C.-76 A.D.)
T-109-7 [†]	4	<1cm charcoal fragments in overlying pf from Irazú	2010 ± 60	36 B.C.–1 A.D. (87 B.C.-63 A.D.)
T-27-b-10	4	Outer 4 cm of a 15–20-cm-thick peat log in fallout deposit	2330 ± 90	397 B.C. (479–260 B.C.)
5-2-89*	5	Small charcoal fragments in base of overlying soil	2495 ± 135	760–560 B.C. (802–401 B.C.)
T-26-b-10	5	Small charcoal fragments in base of overlying soil	2590 ± 180	796 B.C. (905–409 B.C.)
1-6-89*	5	Small charcoal fragments in base of overlying soil	2705 ± 85	831 B.C. (966–800 B.C.)
11-9-89*	6	Small charcoal fragments in underlying soil	2995 ± 215	1258–1218 B.C. (1493–917 B.C.)
4-10-89*	6	Small charcoal fragments in underlying soil	3115 ± 140	1406 B.C. (1520–1133 B.C.)
T-80	8b	1–3 cm charcoalized wood fragments in pf	8250 ± 300	7314–7203 B.C. (7514–6826 B.C.)

*Analyzed at Krueger Enterprises.

[†]Analyzed at USGS Radioanalytical Laboratory; all others at Teledyne Isotopes.

[§]Best fit calendar ages using the correction curves from Stuiver et al. (1998). Ages in parentheses represent the maximum and minimum ages defined by 1σ total error.

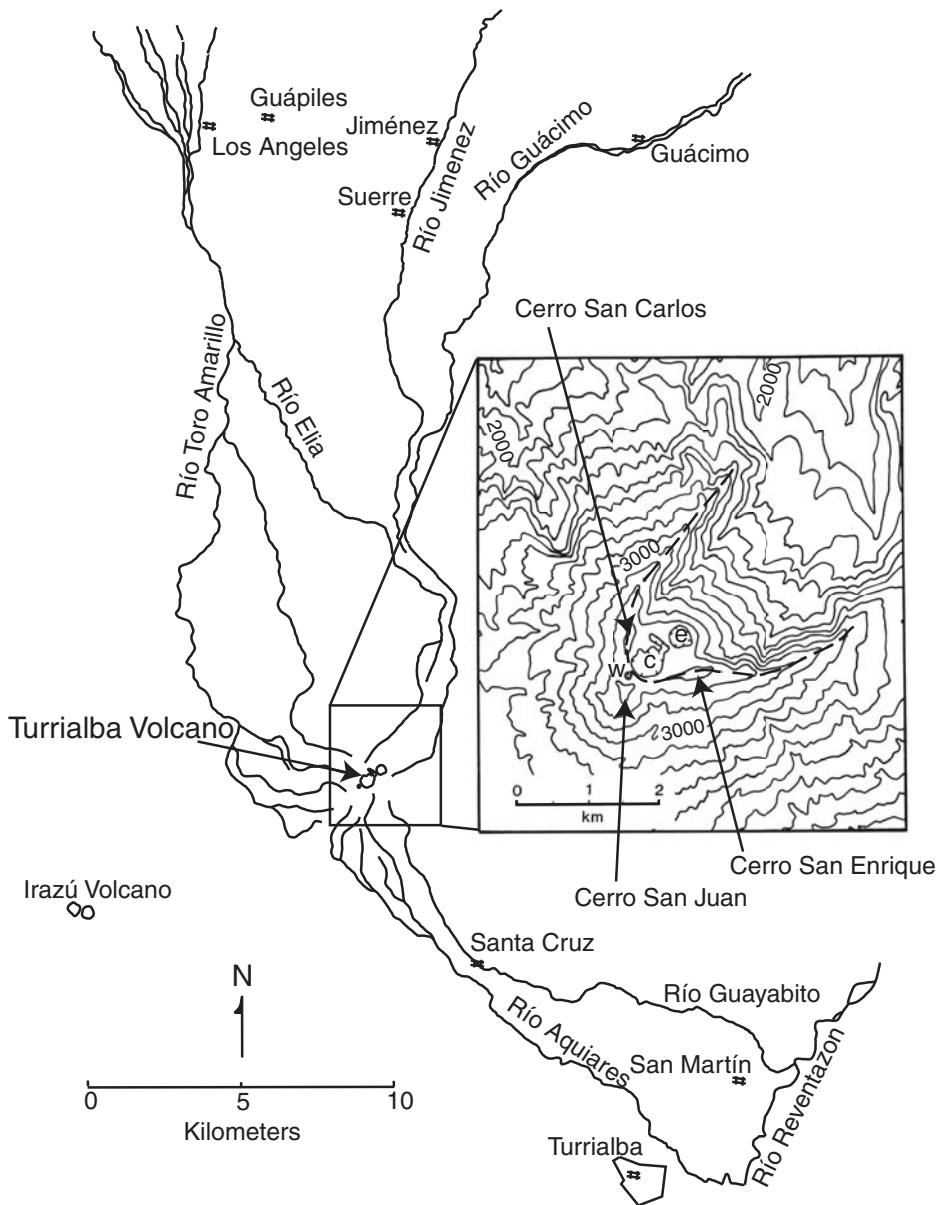


Figure 2. Regional sketch map of geographic features near Turrialba volcano, including cities (indicated by number signs) and major drainages. The inset is a topographic map of Turrialba's summit region. Contours are in 100 m intervals. The rim of the erosional valley is outlined with a dashed line. The three craters of Turrialba's summit are marked (w) for the west crater, (c) for the central crater, and (e) for the eastern crater east craters. Also labeled are the three summit peaks of Turrialba.

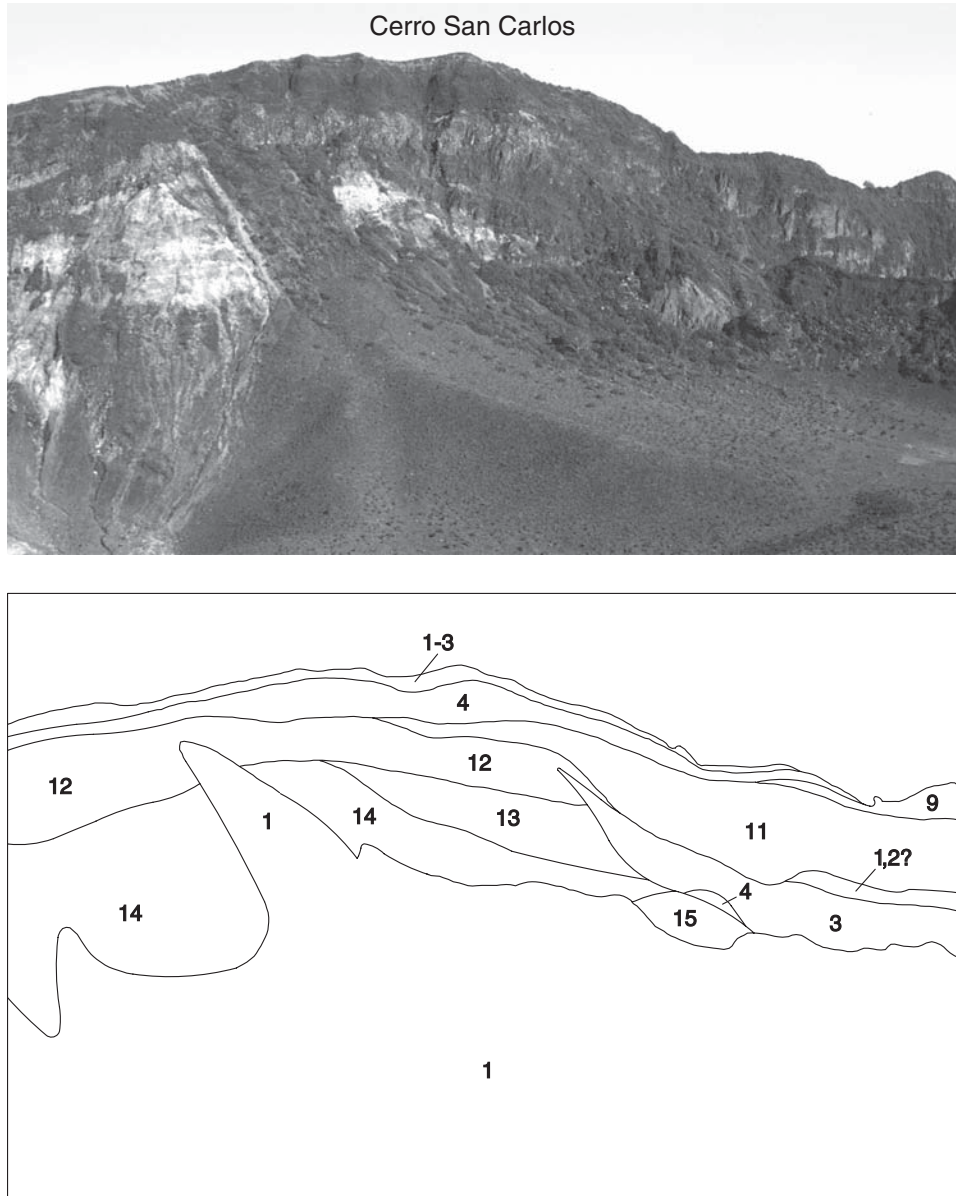


Figure 3. Photograph and sketch of the northwest wall of crater c. Perspective is from the southern rim of crater c. Unit numbers are labeled on the sketch maps.

Medium-K silicic andesite (57–59 wt% SiO_2) lavas of unit 9 make up the majority of the crater walls beneath Cerro San Enrique, as well as the ridge-crest to the northeast of Cerro San Juan (Fig. 4). Another outcrop is found ~300 m south-southwest of crater w. The presence of outcrops on three sides of Turrialba's erosional valley indicates that this eruption was one of Turrialba's most voluminous and that it built a tall central summit cone. The minimum age for this unit is the 9300 yr B.P. age assigned to unit 8. The maximum age for this lava is ca. 50,000 yr B.P. based on a K-Ar age that is indistinguishable from zero (J.B. Gill, 1986, personal commun.).

Much of the northeast side of Turrialba (~1 km³) was removed by erosion between the eruptions of units 9 and 8 (i.e.,

between 50,000 and 9300 yr B.P.). The embayment formed by this erosion resembles a debris avalanche crater (Fig. 2). However, a major debris avalanche deposit has not been identified on the laharic plane to the north of Turrialba volcano, suggesting that the embayment was produced by a different mechanism and/or in piecemeal fashion by a number of mass wasting events.

The time constraints on the erosional period coincide with the Chirripó and Talamanca glacial episodes of Costa Rica's Cordillera de Talamanca, 50–80 km south to southeast (Orvis and Horn, 2000; Lachniet and Seltzer, 2002). Extrapolation of Turrialba's present-day slopes toward a central peak indicates that its former elevation could have been >3500 m before erosion. This height may have been sufficient to allow ice accumulation

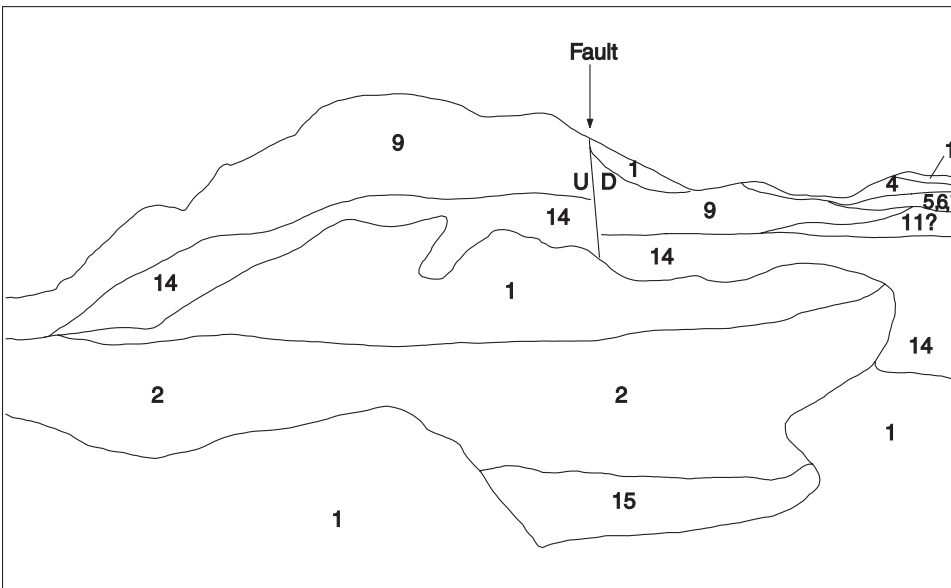
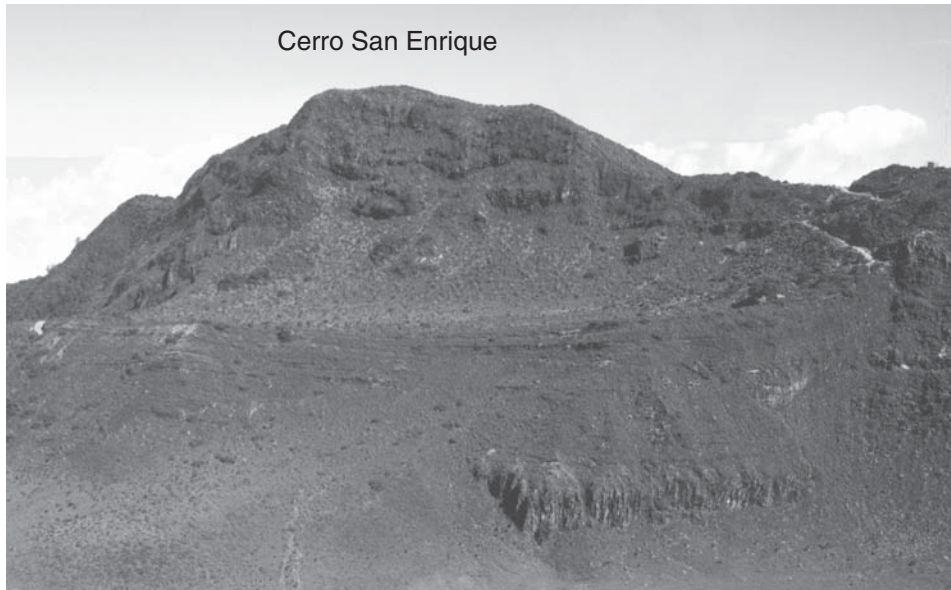


Figure 4. Photograph and sketch of the southeastern wall of crater c. Perspective is from the west rim of crater c. Unit numbers are labeled on the sketch maps. U and D indicate the relative movement on the crater wall fault.

during the maximum Talamanca (Lachniet and Seltzer, 2002) or Chirripó IV (Orvis and Horn, 2000) glacial events, which had equilibrium line altitudes as low as 3300 m in the Cordillera de Talamanca. Therefore, the horseshoe-shaped morphology of the crater rim may have begun as a cirque that was carved by ice into the northeast-facing slope of a peak centered near the location of crater c before 12,000 yr B.P. (see Orvis and Horn, 2000). Following this glacial erosion, subsequent slope failures, including one significant enough to leave a hummocky deposit within the Río Elia–Río Guácimo valley ~3 km northeast of crater e (Soto, 1988), and stream erosion widened and deepened this valley.

The first eruptions after the erosional period produced three large lava flows of high-K silicic andesite and dacite. These flows

have been grouped into unit 8 (Fig. 7). The oldest of these lavas is an olivine-augite-orthopyroxene silicic andesite (subunit 8a) that is exposed along the Río Guácimo and a dacite (subunit 8b) that flowed through the mouth of the Río Elia–Río Guácimo valley and forms a 200-m-ridge 12 km to the north of Turrialba’s crater complex. A dacitic pyroclastic flow overlying the outcrop of unit 9 southwest of crater w may be the stratigraphic equivalent of subunit 8b. If so, then subunit 8b erupted ca. 9300 yr B.P. based on a radiocarbon age of 8250 ± 300 yr (Table 1) corrected to calendar years using the method of Stuiver et al. (1998). Massive lava flows of 57–58 wt% SiO₂ hornblende-orthopyroxene-augite-olivine andesite overlie these two lavas and make up the northeast and east walls of crater e (subunit 8c, Fig. 5). These

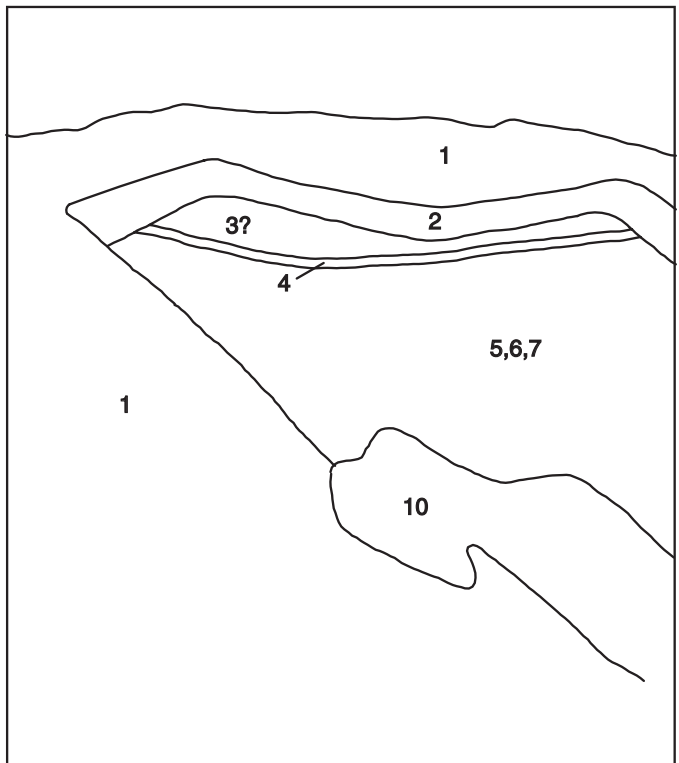
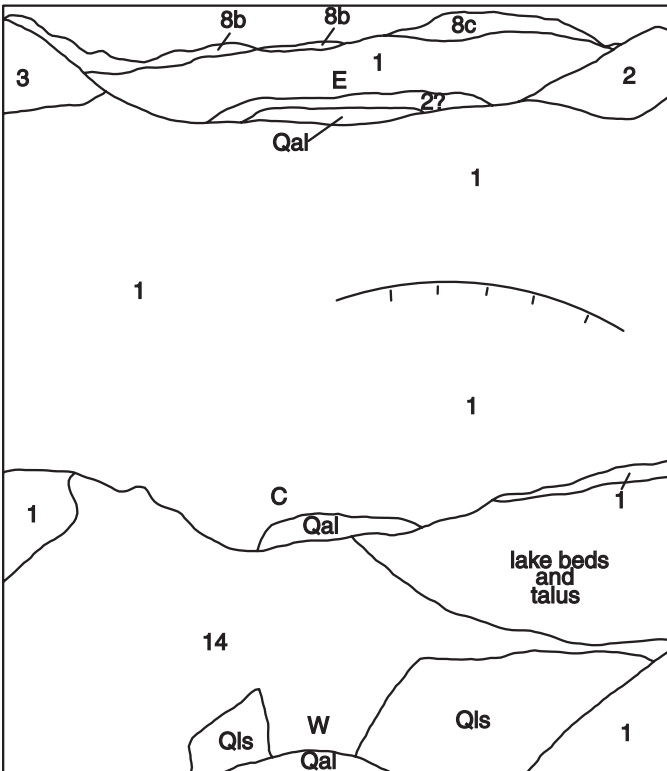
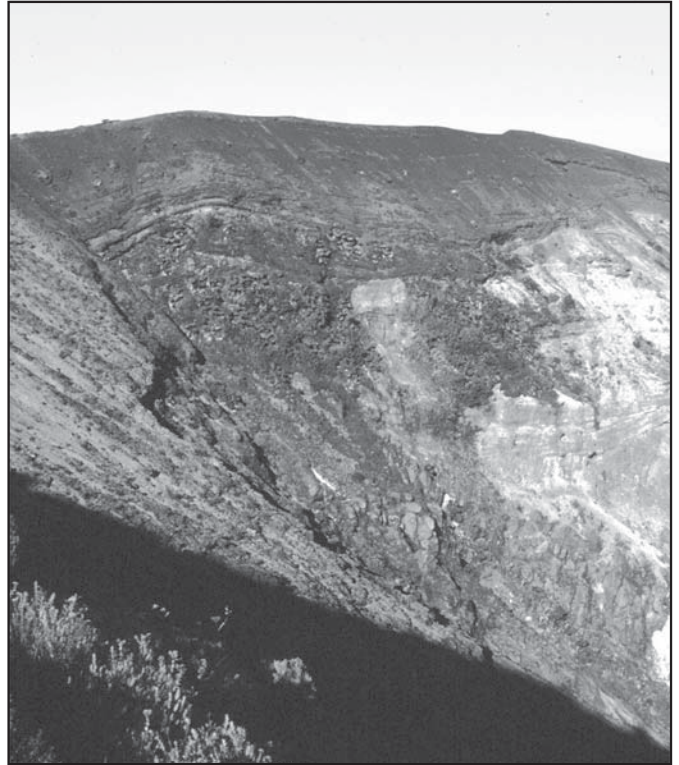
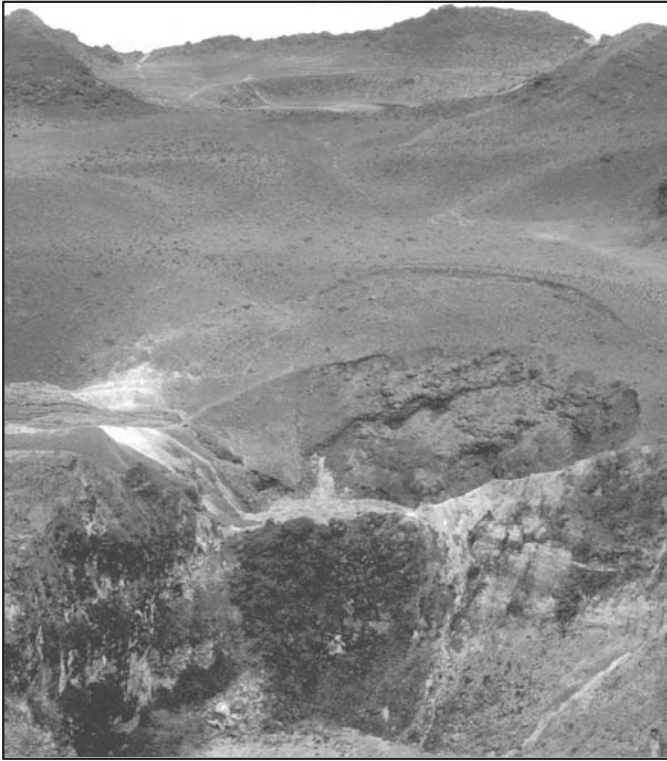


Figure 5. Photograph and sketch of Turrialba's craters. C—central crater; E—east crater; W—west crater. Perspective is from the southwest rim of crater W. Unit numbers are labeled on sketch maps. Qal—Quaternary alluvium; Qls—Quaternary landslide.

Figure 6. Photograph and sketch of the south side of crater w. Perspective from its east rim. Unit numbers are labeled on the sketch maps.

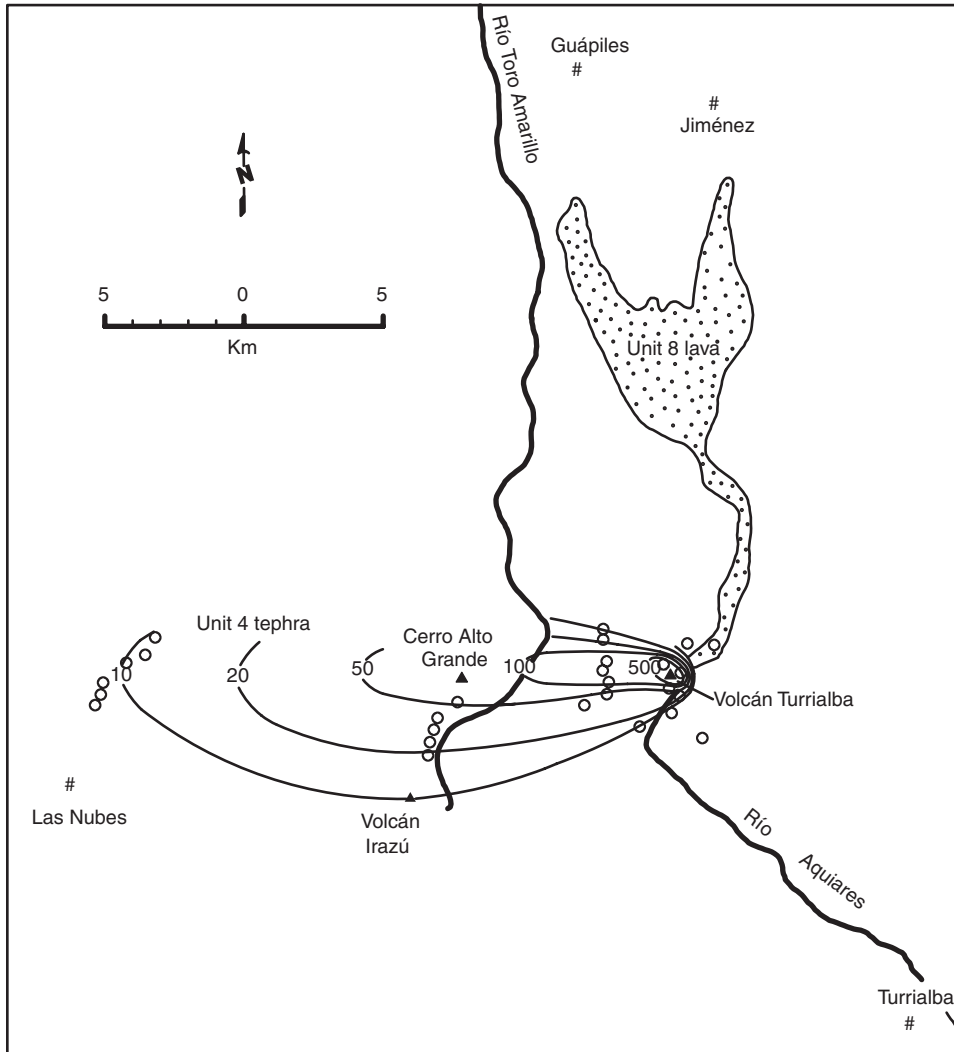


Figure 7. Distribution of unit 4 fallout tephra (thickness in cm) and unit 7 lavas (stippled). Small filled circles show tephra sites.

flows erupted from a vent that was located in what is now crater e and flowed down the northeast-facing valley and eventually traveled up to 20 km from the vent (Fig. 7), where flow-fronts are 60–80 m tall. The total volume of unit 8 is at least 4.5 km³, based on the assumption that its thickness averages a minimum of 150 m. This is one of the largest lava flow complexes recorded in Central America, and may have been the result of magma ponding and differentiation during the erosional era followed by rapid extrusion of the stored magma once the glacier and summit area was removed.

A fundamental change in Turrialba's eruptive style occurred between the eruptions of units 8 and 7. Whereas the eruptions of unit 8 produced relatively large-volume andesite to dacite lava flows, succeeding eruptions were more predominantly explosive and, with the exception of unit 4, were generally less silicic. Although tephra deposits from these eruptions are relatively widespread, the associated lavas are confined to the interior of Turrialba's crater complex.

Unit 7 consists of basaltic andesitic (~56 wt% SiO₂, see Table A1) scoria in pyroclastic fall and surge beds that underlie unit 6 on the south side of crater c (Fig. 4). This scoria consists of red to dark gray augite-olivine basalt and contains <1 cm blebs of porphyritic dacite pumice. This dacite may have been the last remnant of the silicic unit 8 magmas flushed from the system by eruption of the basaltic andesite. Charcoal from an overlying soil horizon exposed in a road cut below the radio tower on Turrialba's southeast side was dated at 2995 ± 215 radiocarbon years (Table 1), which corrects to a calendar age of ca. 3200 yr B.P. Thus, the minimum age of unit 7 is 3200 yr B.P. Ash found within a peat deposit 35 km northeast from Turrialba volcano at El Silencio has a radiocarbon age of 3370 yr B.P. (Obando and Soto, 1993) and may be the equivalent of unit 7.

On the southeast rim of crater c, unit 6 consists of interbedded well to moderately sorted and laminated dark gray juvenile ash and poorly sorted ash, lapilli, and block deposits with dense juvenile clasts up to 1 m in length. On Turrialba's flanks (Fig. 8),

the base of the deposit consists of yellow clay that originally was phreatic explosion debris. Overlying this are weakly to highly weathered gray to dark gray fine to coarse juvenile ash deposits. Where undisturbed, these deposits are usually finely bedded and rarely cross-bedded. Juvenile clasts are olivine-augite basalt or basaltic andesite, with minor augite-orthopyroxene silicic andesite to dacite and hybrids of these two compositions. Well-developed orange-brown soil horizons underlie and overlie this deposit. The maximum age of unit 6 is 3400 yr B.P. based on the 3115 ± 140 yr B.P. radiocarbon date of charcoal fragments from the underlying soil horizon (Table 1). The minimum age of unit 6 can be estimated by the age of the soil atop unit 5.

Unit 5 comprises thin, poorly-sorted ash and lapilli deposits found on Turrialba's upper flanks (Fig. 9). This deposit is highly weathered, consisting of dense angular andesitic lapilli in a light gray to tan clay matrix, and probably was deposited by pyroclastic flows or surges. No well-sorted deposits clearly related to ash fallout were observed, although such deposits may have been obscured by weathering. Charcoalized wood fragments <2 cm in length from the base of a well-developed soil that overlies unit 5 were dated between 2705 ± 85 and 2495 ± 135 radiocarbon years (Table 1). The charcoal's location at the base of the soil suggests that it was produced in the eruption or from a fire relatively shortly after eruption. Thus, the best estimate for the calendar year age of unit 5 is a calibrated age based on the oldest of these radiocarbon ages, ca. 2800 yr B.P., and the maximum repose time between unit 5 and 6 was ~600 yr.

Unit 4 consists of air fall, surge, and pyroclastic flow deposits of high-K, 58–59 wt% SiO₂ andesite that erupted from a vent in the vicinity of crater c. This andesite can be distinguished from those of other units by its abundant phenocrysts (30%) of plagioclase, dark green augite, orthopyroxene, and rare olivine in frothy pumice, and its relatively high SiO₂ concentrations. It is useful as a marker horizon for central Costa Rica (see Clark et al., this volume). The deposits are up to 40 m thick on Cerro San Carlos, 1.3 m thick 2.5 km from the summit, and 0.1 m thick ~20 km west of Turrialba (Fig. 7). Pyroclastic flow and surge deposits from this same eruption overlie the fallout deposit on the south and west flanks of Turrialba. Radiocarbon ages of the fallout and pyroclastic-flow deposits range from 2330 ± 90 yr B.P. to 1860 ± 100 yr B.P. The most precise date (1975 ± 45 yr B.P.) is from a 3-cm-thick charcoalized branch found in fallout pumice near the summit of Turrialba. The most likely calendar age of this branch and the fallout deposit is ca. 1970 yr B.P. (see Table 1). Melson et al. (1985) report a similar radiocarbon age (1970 ± 90) for a phreatic explosion layer that is overlain by a pumiceous fall deposit and underlain by a paleosol bearing 2000 yr B.P. ceramic fragments. Therefore, the repose time between the eruptions of units 4 and 5 was ~800 yr.

On the east rim of crater c, unit 4 comprises interlayered buff, gray, and dark-gray beds consisting almost entirely of angular clasts of juvenile siliceous andesite up to 40 cm in length (Fig. 10). The buff layers are poorly sorted to well-sorted, consisting of lapilli and blocks of juvenile pumice, with lesser amounts

of dense, dark gray juvenile clasts (5%–15%) and altered volcanic lithics (<5%). Large pumice blocks grade outward from a dark-brown core through a 1–5 cm pink zone to a 1–3 cm thick buff rim (Plate 1). This pumice is interbedded with gray, poorly sorted layers of dense to coarsely vesicular juvenile clasts and minor altered lithic fragments.

Downwind to the west, along the crest of the fallout dispersal pattern, and within 1–10 km of the summit, unit 4 is normally graded overall and consists of 4 layers, labeled A–D from bottom to top (Fig. 10; Plate 2). Layer A is well-sorted, normally graded, and is mostly buff pumice lapilli with subordinate amounts of dark gray, dense juvenile clasts and accidental ejecta. Within 2 km of the summit, thinly bedded surge deposits of gray ash sometimes underlie layer A. The base of layer B usually consists of <1 cm of fine pink ash. Most of layer B is moderately sorted, weakly bedded, medium gray, and consists of buff pumice lapilli and gray ash. Layer C is like layer A but is finer-grained. Layer D is a moderately sorted gray ash that contains sparse pumice lapilli. Farther downwind, near the town of Las Nubes, unit 4 consists of one well-sorted bed consisting of lapilli and coarse ash with a distinctive salt-and-pepper appearance. On Turrialba's east, west, and south flanks, and within 3 km of the vent, the fallout tephra of unit 4 are usually overlain by interbedded pyroclastic flow and surge deposits from the same eruption (Fig. 11).

The minimum volume of the fallout deposit was calculated to be 0.2 km³ using the method of Pyle (1989) and the contours shown in Figure 7. Adding the over-thickened proximal fallout deposits and the relatively minor volumes of pyroclastic flows and surges associated with this eruption would bring the total volume to no more than about double this amount.

The pyroclastic deposits of unit 3 overlie a well-developed soil horizon atop unit 4 (Fig. 12). This soil contains charcoal dated at 1630 ± 160 radiocarbon years by William Melson (1990, personal commun.). On the west rim of crater c, unit 3 has a buff to tan basal portion, which is massive and poorly sorted at its base and moderately sorted and well-bedded on top. Overlying this is a dark gray upper portion that consists of interbedded near-vent, surge, and fallout deposits, with the proportion of fallout deposits increasing down-section. Greater than 20 m of gray near-vent pyroclastic deposits make up unit 3 in northern crater c, at the head of the Río Elia (Fig. 12), suggesting that pyroclastic surges of unit 3 may have flowed down the Río Elia Valley. On the western rim of crater c, the lowermost juvenile clasts consist of white bands of nearly pure dacite intermingled with black bands of a 60% basaltic andesite–40% silicic andesite mixture. Juvenile clasts in overlying deposits are mostly basaltic andesite.

On Turrialba's flanks, unit 3 has a yellow to tan base entirely consisting of highly altered volcanic clasts (Plate 3). The base generally makes up one-third to two-thirds of the total deposit and usually is massive and poorly sorted, although moderately well-sorted and laminated strata with rare cross-beds are occasionally present. The overlying beds are dark gray and massive to planar with rare cross-beds and consist of moderately to well-sorted mostly juvenile basaltic andesite ash. An orange- to

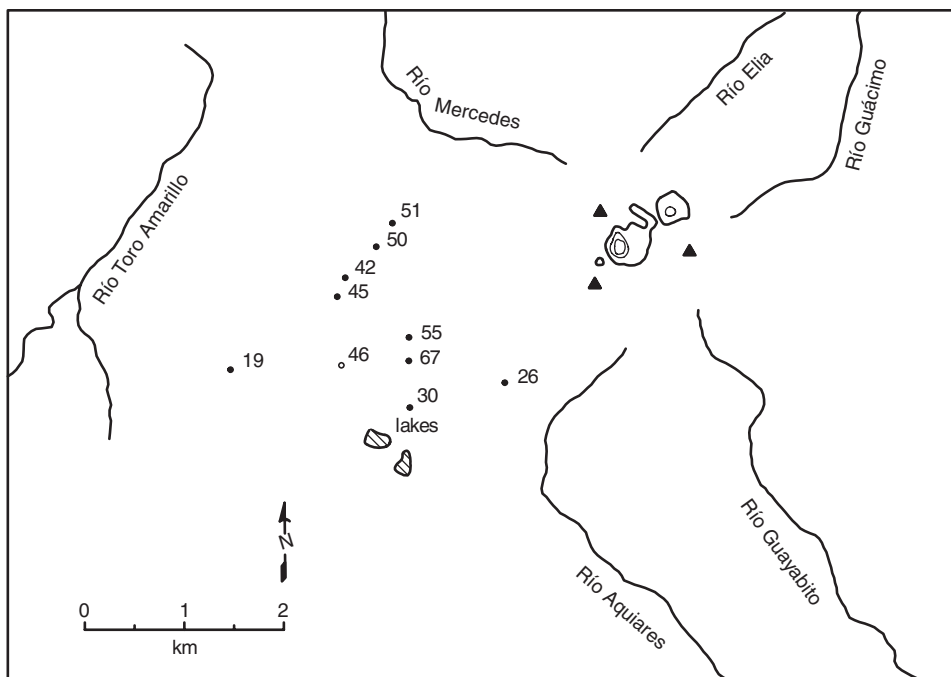


Figure 8. Thicknesses of unit 6 pyroclastic deposits in centimeters.

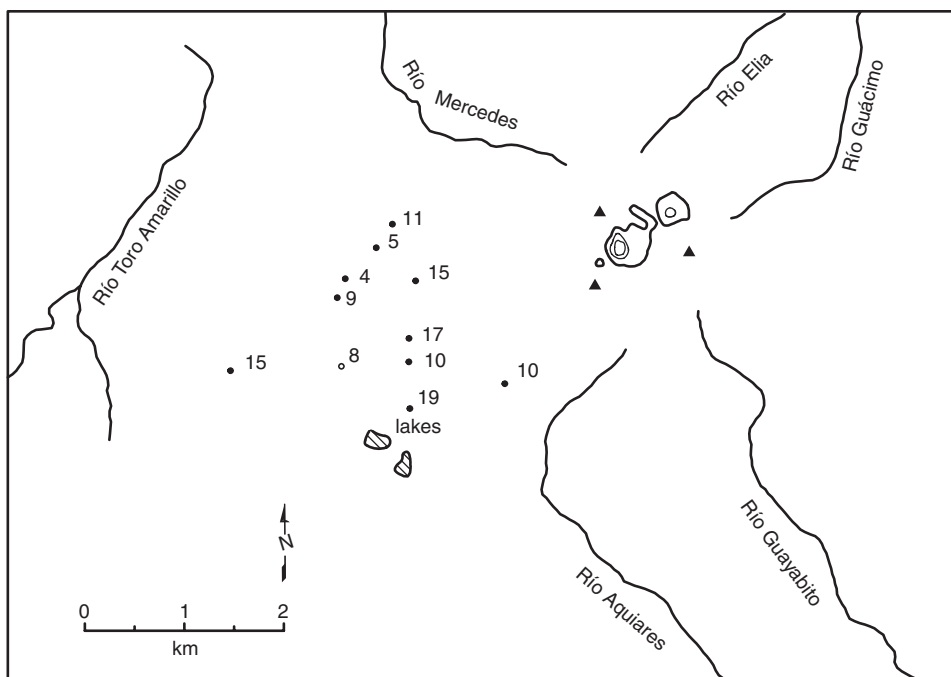


Figure 9. Thicknesses of unit 5 pyroclastic deposits in centimeters.

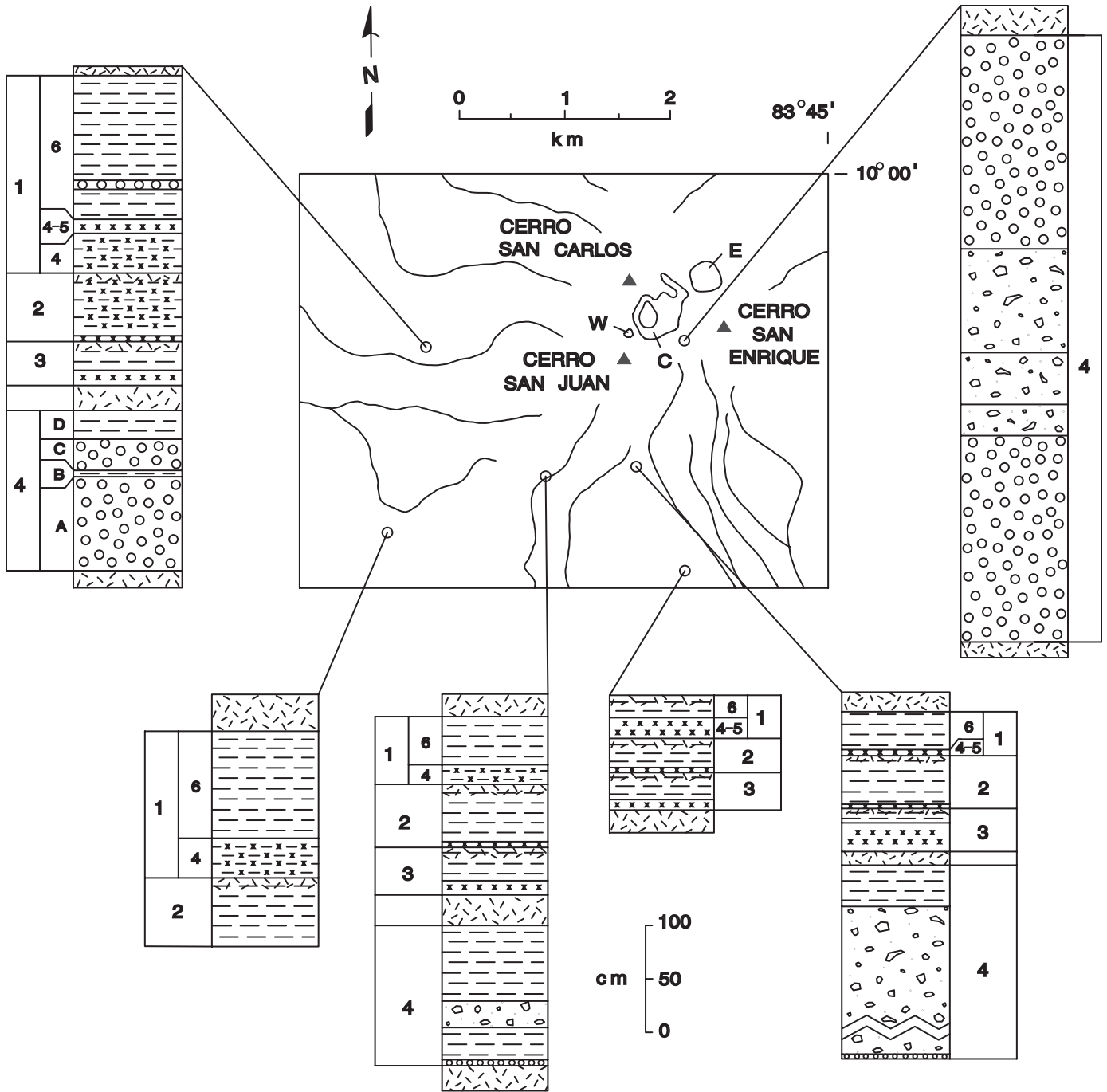


Figure 10. Tephra stratigraphy at representative sites. Unit numbers are listed next to stratigraphic columns. Fallout tephra with juvenile pyroclasts are shown by fields of open circles. Well-bedded pyroclastic surge and fallout deposits with juvenile clasts are shown by fields of horizontal dashed lines. Similar deposits, but with mostly nonjuvenile clasts are shown by fields of dashed lines and x's; x's alone represent poorly sorted deposits of nonjuvenile debris. Fields with randomly oriented angular forms are pyroclastic flow deposits. Randomly oriented dashes represent soil horizons. Subdivisions within unit 1 represent the estimated dates of eruption: 4 = 1864; 4-5 = 1864-1865; 6 = 1866. Subdivisions A-D for unit 4 are described in text. C—central crater; E—east crater; W—west crater.

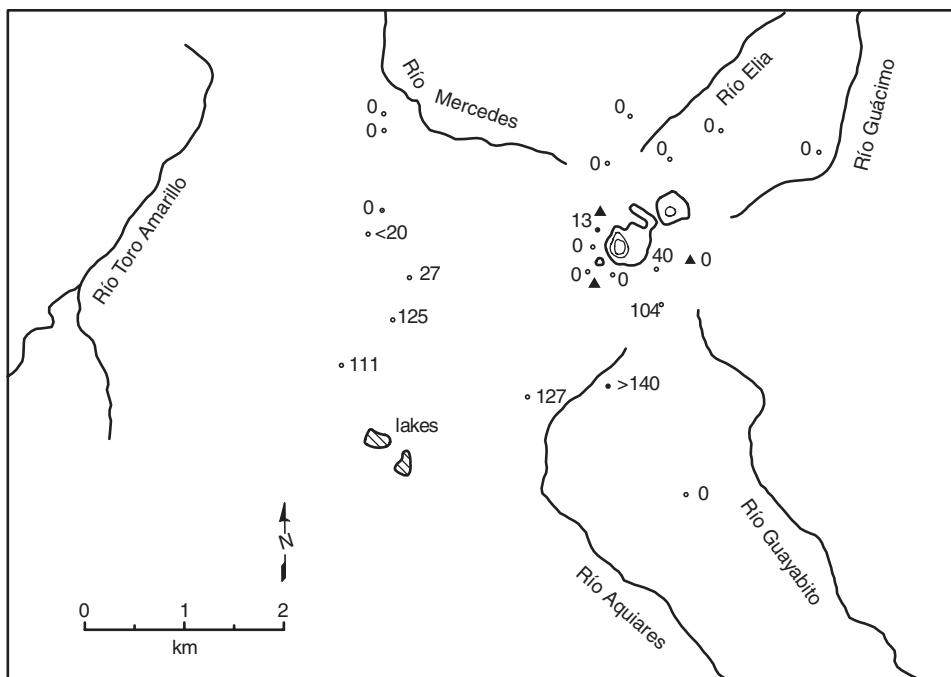


Figure 11. Thicknesses of unit 4 pyroclastic flow and surge deposits in centimeters.

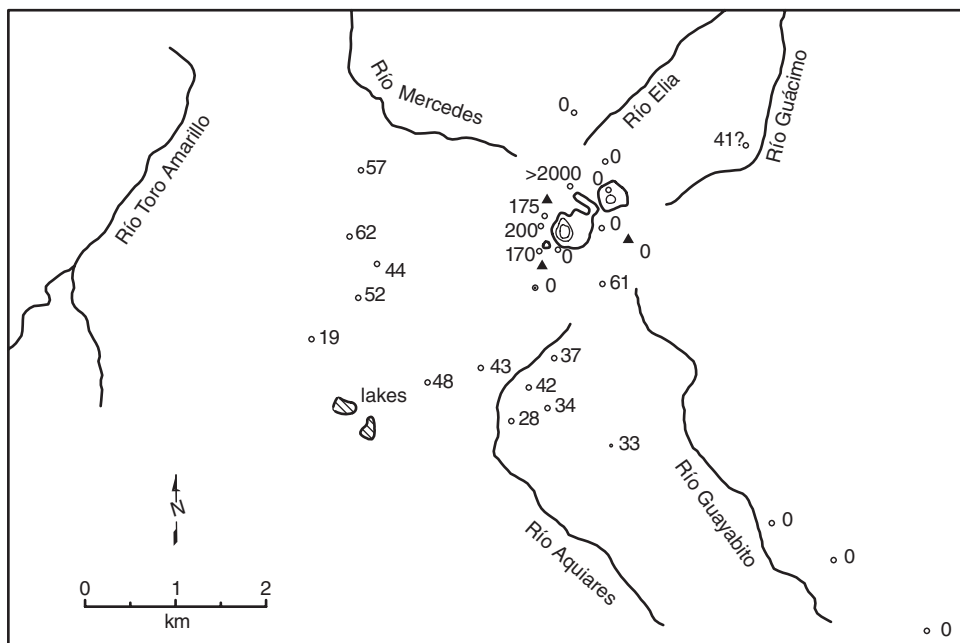


Figure 12. Thicknesses of unit 3 pyroclastic deposits in centimeters.

red-brown soil that is typically thinner than the underlying soil caps unit 3.

A 10 cm thick peat log found within the basal nonjuvenile surge beds of unit 3 yielded a radiocarbon age of 1415 ± 75 (Table 1), which corrects to a calendar age of ca. 1360 yr B.P. (Stuiver et al., 1998). Thus, the repose time between the eruptions of units 3 and 4 was ~600 yr.

Within Turrialba craters, pyroclastic deposits of unit 2 overlie unit 3 in the southeast wall of crater e and the south wall of crater w and unit 15 in the east inner wall of crater c (Figs. 5, 6, and 13). The deposits are generally well-bedded, well-sorted to poorly sorted, and buff to gray. Nonjuvenile, variably altered volcanic clasts dominate most beds. Nevertheless, juvenile basaltic andesite clasts are found in exposures around craters c and e. Where bedding is well-preserved, unit 2 is moderately to well sorted and well bedded, and has rare cross beds. The upper 5–20 cm usually has a pervasive pale orange tint and some more deeply orange horizons and veins (Plate 3). This likely represents a weakly developed soil and suggests that the repose time between the eruptions of units 1 and 2 is significantly less than the intervals between the eruptions of units 2–6.

Unit 1, which erupted in 1864–1866 A.D., mantles most of Turrialba's summit region (Fig. 14). Juvenile lavas and pyroclasts of unit 1 are 52.5–53 wt% SiO_2 basalt (see Table A1). On the floor of crater c, unit 1 comprises agglutinates and rootless lava flows overlain by surficial fallout and near-vent flowage deposits. On the crater rims, it consists of alternating beds of well-sorted to poorly sorted pyroclastic deposits (Plate 4). Its thickness is highly irregular, reflecting syn- and post-eruption erosion, as well as variable depositional thickness. Its base often consists of poorly sorted deposits of ash- to block-sized clasts of buff to yellow altered volcanic rock. Overlying deposits are well bedded and poorly to well sorted, with the proportion of juvenile clasts increasing up-section. Some of these beds are indurated and vesicular, and some have low angle cross beds. About 10%–30% of the sections along Turrialba's crater rims consist of open-network well-sorted ash or lapilli deposits. Within 200–500 m of crater w, the uppermost layer is a fallout deposit of highly altered volcanic debris that erupted from crater w.

Outside of the crater, to the east of the Turrialba crater complex, the base of unit 1 consists of buff to yellow ash and lapilli of altered volcanic debris. Most of this deposit is poorly sorted, but some well-sorted ash beds are present. To the west and south, the base of unit 1 is a varicolored horizon consisting of interlayered yellowish and light to dark gray beds made up of more and less altered volcanic clasts. The top of this bed often has some discontinuous orange-stained horizons. This is overlain by a thin, poorly sorted yellowish deposit rich in nonjuvenile clasts. The upper of two-thirds to nine-tenths of unit 1 consists of plane parallel layers of moderately to well-sorted ash with rare cross beds (Plate 5). Some of these beds are indurated and vesicular. Cross bedding is particularly conspicuous in deposits associated with topographic lows (Plate 6). The ash in these beds is mostly juvenile basalt with 10%–40% nonjuvenile volcanic debris. One well-sorted

fall bed composed of scoria lapilli is present in sections to the west and southwest of Turrialba's summit. Poorly sorted deposits <2 m thick that likely represent lahars from the 1864–1866 eruption are found in patches along the banks of the Río Aquireas near the town of Aquireas and along the Río Guacimo and Río Roca valleys 7 km north of Turrialba's summit.

Although the thicknesses of units 1, 2, 3, 5, and 6 are highly irregular, they appear to be similar to or less than the thicknesses measured at similar distances for basaltic tephra erupted in 1963–1965 from Irazú volcano. Thus, all of these units probably have volumes $\leq 0.03 \text{ km}^3$, which is the estimated volume for the 1963–1965 eruption (Clark et al., this volume).

THE 1864–1866 ERUPTION

The following discussion is our interpretation of the 1864–1866 eruption sequence based mostly on the eyewitness accounts reported in González-Viquez (1910). Following a period of enhanced fumarolic activity beginning on or before 1723 A.D., Turrialba began erupting significantly on 17 August 1864 and continued erupting until at least February 1866.

On 26 February 1864, an expedition to Turrialba found a summit region with an active crater >100 m deep with more than 100 fumaroles in its walls and bottom (see Figs. 2 and 10). This may have been a precursor to today's crater w. The interior four walls of the crater were steep and black to yellow and white in color. The west crater wall and crater floor were intensely altered, and the west crater wall was hot to the touch. No vegetation was present within the crater area, and much of the vegetation to the west and northwest was dead because of acid rain. Areas near the fumaroles were covered with sulfur. The vapors from all of the fumaroles combined and rose ~200 m above the summit. The accounts suggest that the summit had two "dead" craters, one to the east and one to the northeast. These probably correlate to the area occupied by craters c and e today.

The explosive eruption of Turrialba began on 17 August 1864. Ash fell on Costa Rica's Central Valley throughout 16–21 September, and ash was detected as far west as Atenas and Grecia. Enough ash fell in San José that it caused alarm and could be scooped up for a chemical analysis, but apparently not enough to cause major hardship. The thickness of ash in San José, therefore, was probably less than ~2 mm.

A second expedition trekked past a lake with more than a third of a meter of ash nearby and reached Turrialba's summit on 30 September 1864. Although the location of the lake is not well described, the only lake close enough to Turrialba's summit to have received this much ash is a transient lake 3 km southwest of crater c. A stratigraphic column of unit 1 from the lake area (Fig. 10) shows a 36-cm-thick varicolored basal unit bearing cross-beds that may correspond to the deposit seen by the expedition.

The summit region and the fumarolic activity had changed substantially since the first expedition. Where there were 100 fumaroles before, there was now one, which was a belching green



Plate 1. Clasts in unit 4 near radio tower at Turrialba's summit.

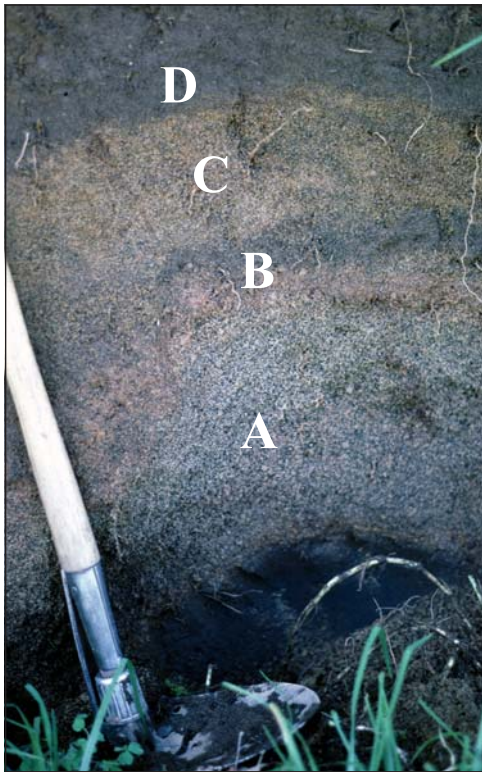


Plate 2. Downwind stratigraphy of unit 4. Subdivisions A–D for unit 4 are described in text.

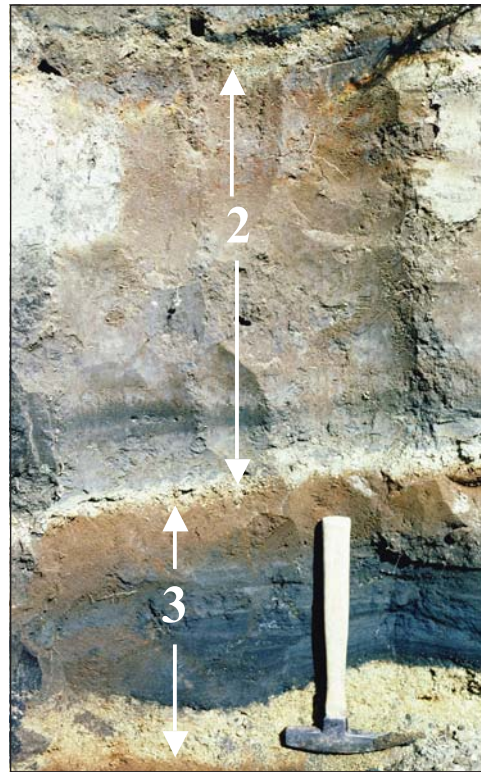


Plate 3. Units 2 and 3 in roadcut 2 km south of Turrialba's crater complex.

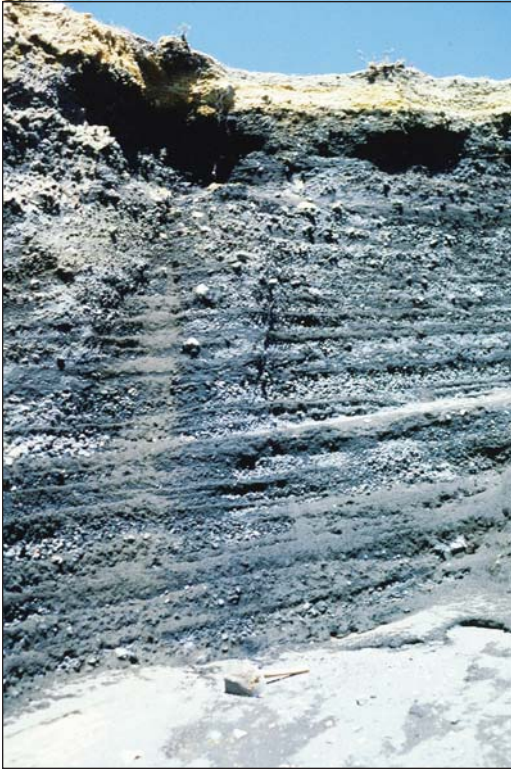


Plate 4. Unit 1 near rim of crater w.

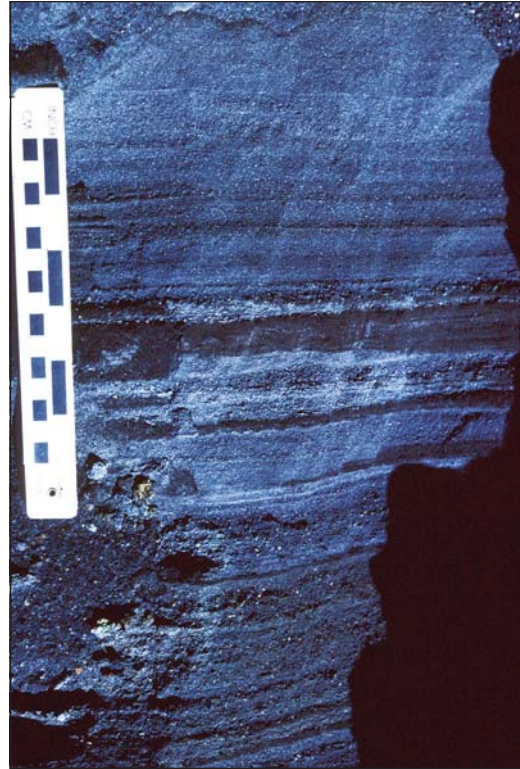


Plate 5. Unit 1 tephra in roadcut 2 km west of Turrialba's crater complex.

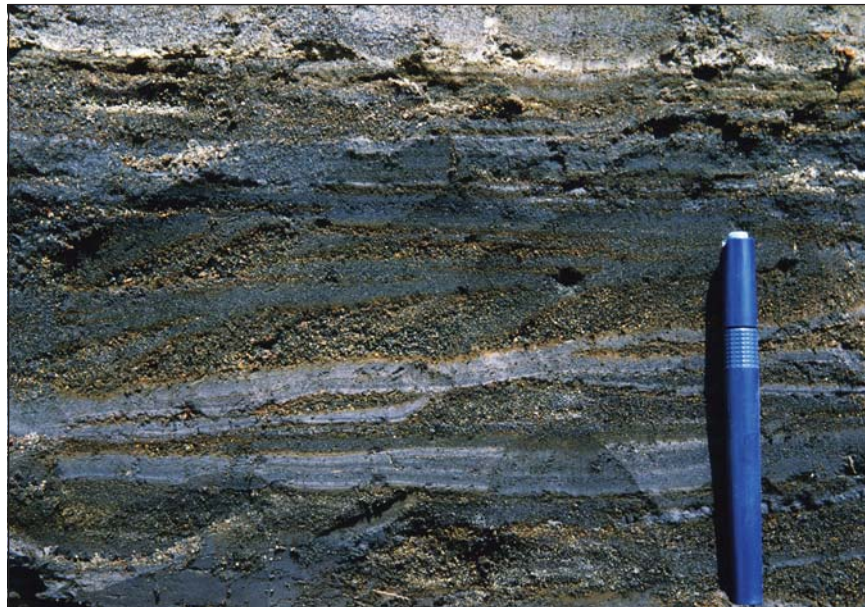


Plate 6. Cross-bedding in unit 1.

to black plume about twice as tall as the one seen during the first trip. Blue flames, possibly from the burning of sulfur, were associated with this plume. The roar of this vent was very loud, and the mountain was continually shaking. Part of the summit was missing, and it was suggested that it fell into the new crater and was thrown back out as ash. A lot of this ash apparently went to the north and northwest. Large blocks lay on the surface in the entire summit region. Vegetation was destroyed between Turrialba volcano and near where the Río Tortuguero (now named the Río Toro Amarillo) starts, and for many kilometers to the northwest and west of Turrialba volcano.

It appears that after the 16–20 September eruption, there was still only one active crater (crater w), but it had been significantly widened. This excavated material was deposited to the north, south, and west of the volcano by ash fallout and pyroclastic surges. It is likely that little magma was involved in this part of the eruption and that the lowermost varicolored beds of unit 1 found west and southwest of Turrialba are associated with this eruption.

A third expedition visited Turrialba on 9 March 1865 after more ash had fallen on San José during late 1864 to 8 March 1865 (von Seebach, 1865). This expedition found a widened westernmost crater with a funnel shape like today's crater w. The additional material excavated from crater w was probably deposited as the yellow to tan beds overlying the varicolored beds in unit 1. Although this expedition observed some bombs near the craters, it is likely that juvenile pyroclasts still did not make up a significant proportion of the ejecta.

Eruptions in January and February 1866 were apparently the largest of the 1864–1866 eruptive period. Ash fell in the Central Valley for four days in January and three days in February, and fell as far as Puntarenas (125 km away) ca. 1 February. The juvenile-clast-rich upper portions of unit 1 probably erupted during this period, including the thick scoriaceous deposits on the south side of crater w and the rootless lava flows and agglutinates on the floor of crater c. Most of the material probably erupted from the interior crater of crater c. Two concentric tephra rings that run along the northeastern floor of crater c show that the vent crater was larger and located farther east during early stages of the eruption. The distribution of tephra deposits suggests that much of the area within 5 km of the volcano was buried in thick ash by the eruption. The eruption concluded with a small phreatic explosion from crater w.

In summary, the most recent eruption of Turrialba volcano began on 17 August 1864 and lasted into February 1866. The eruption was entirely explosive. Phreatic explosions from crater w characterized the first year of the eruption. During the final two months of eruption, juvenile basalt was expelled in phreatomagmatic eruptions from crater c, followed by a last phreatic explosion from crater w. The phreatic and phreatomagmatic explosions produced eruption columns that rained ash and lapilli in the Turrialba summit region and downwind to the west. Pyroclastic surges may have occurred in the summit region during the eruption.

TURRIALBA'S PYROCLASTIC DEPOSITS AND ASSOCIATED ERUPTIONS

Internal structures and distributions of many of the deposits from Turrialba volcano indicate that they were deposited by fallout of ash and lapilli. For example, the salt and pepper lapilli beds of unit 4 and the well-sorted scoria beds of unit 1 are good examples of fallout beds. In contrast, the block, lapilli, and ash deposits of unit 4 clearly were deposited by pyroclastic flows and surges. However, the deposits associated with many of the explosive basaltic and andesitic tephra of Turrialba (e.g., the cross-bedded and well-sorted deposits in unit 1) have characteristics that are intermediate between those expected for pyroclastic falls and surges.

Along Turrialba's crater rims, tephra deposits are well bedded with typical thicknesses of 10–50 cm. The beds range from continuous to discontinuous, and sorting is variable. Well-sorted beds composed completely of ash or lapilli are common, as are poorly sorted block, lapilli, and ash beds. Dropstones are commonly present. At distances >1 km from its crater complex, Turrialba's basaltic and basaltic andesitic deposits are bedded on a millimeter to 10 cm scale. They are ubiquitously fine-grained, consisting of moderately sorted to well sorted ash, which suggests that they were ejected by phreatomagmatic explosions (e.g., Fischer and Schmincke, 1984). The bedding is commonly laterally continuous on an outcrop scale, although variations in bedding thickness and low-angle dune- to steep ripple-scale cross bedding is sporadically present (Plate 6). Some well-sorted ash beds are friable, but many beds are indurated, and some of these consist of coarse ash fragments coated with fine ash. These beds are commonly vesicular, indicating the presence of condensed water during deposition. In contrast to typical fallout sequences, which typically are lobate and thicken toward the source and in the downwind (west to northwest) direction, these deposits have more uneven depositional patterns (Figs. 8–14).

The 1963–1965 eruption of basaltic andesite from Irazú volcano (Murata et al., 1966; Krushensky and Escalante, 1967; Alvarado, 1993; Clark et al., this volume) produced pyroclastic deposits that are similar to those of Turrialba and may be good analogues for the recent eruptions of Turrialba. The 1963–1965 eruption was characterized by periodic Strombolian to vulcanian explosions, whose intensities ranged up to a VEI (volcanic explosivity index; Newhall and Self, 1982) of 3 with intervening quiescent periods that varied over day-long to month-long stages (Sáenz et al., 1982; Alvarado, 1989; Simkin and Siebert, 2002; Clark et al., this volume). The eruption began with phreatic explosions that tossed dense blocks more than a kilometer and covered the western flanks of Irazú with ash. Over the succeeding two years, explosions produced fine-grained ash beds similar to those of the mafic eruptions from Turrialba. The frequent heavy rainfalls also generated destructive lahars and floods of ash-choked water. The descriptions of Murata et al. (1966) and Krushensky and Escalante (1967) indicate that most of the laminated ashes erupted in 1963–1965 were fallout deposits. They attributed the

ripples they observed to aeolian processes, although pyroclastic surges produced similar deposits on north side of the volcano (see Hudnut, 1983). The high degree of tephra fragmentation reflects recycling of conduit wall, as well as a high degree of magma-water interaction during the eruption (Alvarado, 1993).

These observations suggest that the majority of the laminated deposits from explosive basaltic and basaltic andesitic eruptions at Turrialba were fallout tephra from vulcanian to Strombolian explosions with a VEI of 3 or less. Their somewhat uneven distributions can be attributed to syneruption erosion. Some of the cross bedding observed in units 1–3 may have resulted from reworking of unconsolidated ashes by wind, sheet-wash, and stream-flow. Nevertheless, the dropstone-bearing cross-bedded deposits found in Turrialba's crater complex were probably associated with pyroclastic surges. Thus, pyroclastic surges did occur during Turrialba's recent eruptions of basalt and basaltic andesite and constitute a risk during future eruptions.

IMPLICATIONS FOR THE POTENTIAL HAZARDS OF TURRIALBA

Beginning in May 1996, seismic activity recorded by a single station installed at the summit of Turrialba in 1990 escalated from 0 to 91 earthquakes per month to a maximum of 2000 earthquakes per month in October 2000. This seismicity included long-period events. From 2000 to 2004, eight additional seismic pulses were documented by a four station local network that was installed in 2000 (Barboza et al., 2000, 2003). This period of enhanced seismicity was accompanied by fumarolic activity that increased in area, flux, and concentration of magmatic constituents in craters c and w. Burned vegetation, opening of ground cracks, small landslides, rock alteration, and soil heating around both craters also has been reported (Fernández et al., 2002). This recent activity and the relatively short repose period indicated by the weakly developed soil between units 1 and 2 suggest that Turrialba may erupt again within the next several years to several decades.

Five of the six most recent significant eruptions, including the last three, ejected $\leq 0.03 \text{ km}^3$ of altered volcanic debris and juvenile basalt or andesite tephra in VEI ≤ 3 explosions from the summit crater complex. The most probable significant future eruption of juvenile magma, therefore, would probably occur from the summit craters and would be of similar volume and type. The presence of relatively young cinder cones on Turrialba's southwest flank shows that eruptions along the crater lineament, but away from the summit, are also possibility. Like past eruptions of Turrialba, the initial phase of renewed activity would likely involve phreatic explosions. These explosions would produce fallout deposits that could significantly blanket areas within 2–3 km of Turrialba's summit with ash and generate pyroclastic surges affecting the summit region. A few millimeters of ash could fall on the Central Valley during these types of eruptions.

Although it is possible that the eruption would end during the phreatic phase, it is likely that a phreatomagmatic vulcanian to

Strombolian phase would follow. Area similar to that affected by the 1864–1866 eruption would be affected by such an eruption. Ash fall would be heavy in the summit area. Downwind to the west, in the area between Irazú and Cerro Alto Grande, $<10 \text{ cm}$ of ash would be expected. In the Central Valley, near San José and Heredia, the ash fall would probably be $<1 \text{ cm}$. Pyroclastic surges would likely accompany an eruption and could affect areas within a few kilometers of the summit. Low-topography areas, such as river valleys, would have the highest risk of pyroclastic surge damage. Mudflows and floods could occur in many of the drainages leading off of the summit, including Río Toro Amarillo, Río Mercedes, Río Elia, Río Roca, Río Guácimo, Río Guayabo, Río Guayabito, and Río Aquiares. It is possible, though unlikely, that the eruption would conclude with lava effusion.

The young tephra deposits of the historically more active Irazú volcano are similar to those of Turrialba. At Irazú, only 10% of historic eruptions have left discernable deposits (Clark et al., this volume), suggesting that many small eruptions with VEI values of 2 or less may have occurred at Turrialba and were not recorded in its stratigraphy. Thus, minor phreatic and phreatomagmatic eruptions associated with shallow magma intrusions that would only affect the summit region of Turrialba are also possible.

Relatively large volumes of silicic andesite tephra (unit 4) and massive silicic andesite and dacite lava flows (unit 8) have erupted since 9300 yr B.P. Thus, destructive eruptions of silicic andesite and dacite are possible at Turrialba. However, the likelihood of such eruptions at Turrialba is lower than for an eruption of more mafic lava, as Turrialba's last two eruptions ejected juvenile basalts and basaltic andesites and the third oldest eruption involved only a minor amount of silicic andesite mixed with basaltic andesite.

A Plinian eruption of a silicic andesite, like that of unit 4, would be significantly more destructive than an eruption of basalt or basaltic andesite. Ash fall in the Central Valley could reach several centimeters. Pyroclastic flows or surges could extend $>10 \text{ km}$ from the summit. Potentially destructive lahars would likely be generated by such an eruption. Large volume lava flows, such as those of unit 8, are also a remote possibility with this type of eruption.

There is a risk of debris avalanching during future eruptions of Turrialba. Features that promote failure of a volcanic edifice and debris avalanching are (1) a steep slope, (2) massive lavas overlying weak pyroclastic substratum, (3) widespread hydrothermal alteration of the core of a volcano (e.g., Reid et al., 2001), (4) the migration of vents in a direction parallel to the axis of the avalanche caldera, and (5) water saturation of the edifice (Siebert, 1984; Siebert et al., 1987; McGuire, 1996). Turrialba has all of these features. Turrialba's northeast side has the greatest danger of failure (Fig. 2) because it has its steepest slope, it is aligned with Turrialba's vents and faults, and has young, dense lavas overlying an altered volcanic core. If such an avalanche occurred, it would flow down the Río Elia–Río Guácimo valley onto the northern plain. Debris avalanches usually travel $\sim 2\text{--}20$ times as far as the

vertical drop (Ui, 1983; Siebert, 1984). The vertical drop at Turrialba would be ~2.5 km. Thus, the region containing Jiménez, Suerre, and Guápiles could be inundated by such an avalanche. Avalanching of the relatively steep southern, western, and northwestern portions of the edifice is also possible. Indeed, Alvarado et al. (2004) documented a 0.75–1.4 km³ debris avalanche down the Turrialba river valley ~17,000 yr ago that resulted from the collapse of the highland between Turrialba and Irazú volcanoes.

Volcanic blasts are often, though not necessarily, associated with debris avalanches (e.g., the 18 May 1980 eruption of Mount St. Helens; Mullineaux and Crandell, 1981), and such an event could occur at Turrialba. If it did, it would probably be in the same direction as the debris avalanche initially, but would not follow topography as closely and could spread out over ridges onto the northern plane for several kilometers.

CONCLUSIONS

At least 20 eruptions of basaltic to dacitic lavas and tephra are recorded in the stratigraphy of Turrialba volcano's summit region. A period of enhanced erosion and apparently diminished volcanism divides this stratigraphy into pre-erosional and post-erosional units. This erosion-dominated period approximately coincided with the Chirripó and Talamanca glacial episodes of Costa Rica's Cordillera de Talamanca. This, the likelihood that Turrialba had a central peak that exceeded 3500 m in elevation before the erosional period and the morphology of its prominent northeast-facing valley suggest that Turrialba may have hosted a glacier during the last glacial maximum.

The first significant eruption of the post-erosional period was marked by the eruption of massive andesite to dacite lava flows at ca. 9300 yr B.P. These lavas flowed down the northeast-facing valley and out onto the laharc plane as much as 20 km from Turrialba's summit. Suppression of volcanic activity during glaciation followed by enhanced volcanism during interglacials has been noted elsewhere and probably results from a change in the stress distribution in the crust due to ice loading (e.g., Hall, 1982; Nakada and Yokose, 1992; McGuire et al., 1997; Glazner et al., 1999). At Turrialba, the removal of a cirque glacier and the upper volcanic edifice could have decreased the vertical component of the stress field between 1 and 5 MPa depending on the size, shape, and positioning of the central summit cone produced by the eruption of unit 9 and glacier. Rebound above the active vent system may have been sufficient to trigger eruption of magma that had ponded and differentiated beneath the tall edifice built by the last pre-glacial eruption.

Six explosive eruptions are recorded in the tephra stratigraphy at Turrialba over the past 3400 yr. Most were small volume (≤ 0.03 km³) phreatic and phreatomagmatic explosive eruptions involving mostly basalt and basaltic andesite. The exception was a Plinian eruption of ~0.2 km³ of silicic andesite at ca. 1970 yr B.P. Repose periods between significant eruptions over the past 3400 yr have principally been in the range of 800–600 yr. However, the weak soil horizon between the second oldest tephra and

the tephra erupted in 1864–1866 A.D., as well as the recent seismicity, fumarolic, and deformational activity observed beneath Turrialba (Barboza, et al., 2000, 2003; Fernández et al., 2002; Mora et al., 2004) suggest that Turrialba may have entered a more active phase.

Then next eruption probably will be similar to the 1864–1866 and other recent basaltic to basaltic andesitic eruptions. Nevertheless, a larger volume and more destructive eruption of silicic andesite also is possible. Turrialba's steep slopes, particularly the northeast slope of the cone filling the erosional valley, could be susceptible to debris avalanching, and Turrialba should be monitored carefully for deformation during any future eruption.

ACKNOWLEDGMENTS

Eduardo Malavassi is thanked for logistical assistance and for translation of González-Viquez (1910). Field assistance by Joe Hill helped delineate eruptive units 5 and 6. Debbie Trimble is thanked for the radiocarbon analyses from the U.S. Geological Survey. Bill Melson is thanked for sharing his unpublished radiocarbon ages. Funding from UNOCAL and the International Program at the University of Iowa for Reagan is gratefully acknowledged. Soto thanks the Universidad de Costa Rica for funding his Turrialba research. Jim Gill is thanked for comments on an early version of this study. This paper benefited greatly from reviews by John Ewert and C. Dan Miller

REFERENCES CITED

- Alvarado, G.E., 1989, Los volcanes de Costa Rica: San José, Costa Rica, Editorial Universidad Estatal a Distancia (EUNED), 175 p.
- Alvarado, G.E., 1993, Volcanology and Petrology of Irazú Volcano, Costa Rica [PhD thesis]: Germany, University of Kiel, XXXV + 261 p.
- Alvarado, G.E., Vega, E., Chaves, J., and Vásquez, M., 2004, Los grandes deslizamientos (volcánicos y no volcánicos) de tipo debris avalanche en Costa Rica, in Soto, G.J., and Alvarado, G.E., eds., La Vulcanología y su entorno geambiental: Special volume, Revista Geológica de América Central, v. 30, p. 83–99.
- Barboza, V., Fernández, E., Martínez, M., Duarte, E., and Van der Laet, R., E., Marino, T., Hernández, E., Valdés, J., Sáenz, R., and Malavassi, E., 2000, Volcán Turrialba: Sismicidad, Geoquímica, Deformación y nuevas fumarolas indican incrementos en la actividad (abstract), in Los retos y propuestas de la investigación en el III milenio (CONINVES): Memoria, Editorial UNED, p. 78.
- Barboza, V., Fernández, E., Duarte, E., Sáenz, W., Martínez, M., Moreno, N., Marino, T., van der Laet, R., Hernández, E., Malavassi, E., and Valdés, J., 2003, Changes in the activity of Turrialba Volcano; seismicity, geochemistry, and deformation: Seismological Research Letters, v. 74, p. 215.
- Bellon, H., and Tourmon, J., 1978, Contribution de la géochronométrie K-Ar à l'étude du magmatisme de Costa Rica, Amérique Centrale: Bulletin de la Société Géologique de France, v. 7, p. 955–959.
- Carr, M.J., Feigenson, M.D., and Bennett, E.A., 1990, Incompatible element and isotopic evidence for tectonic control of source mixing and melt extraction along the Central American arc: Contributions to Mineralogy and Petrology, v. 105, p. 369–380, doi: 10.1007/BF00286825.
- Clark, S.K., Reagan, M.K., and Trimble, D.A., this volume, Tephra deposits for the past 2600 years from Irazú volcano, Costa Rica, in Rose, W.I., Bluth, G.J.S., Carr, M.J., Ewert, J.W., Patino, L.C., and Vallance, J.W., Volcanic hazards in Central America: Geological Society of America Special Paper 412, doi: 10.1130/2006.2412(12).
- Duarte, E., 1990, Algunos aspectos del riesgo volcanico en el Volcan Turrialba [Licenciado en Geografía thesis]: Costa Rica, Universidad Nacional, 123 p.

- Fernández, E., Duarte, E., Sáenz, W., Malavassi, E., Martínez, M., Valdés, J., and Barboza, V., 2002, Cambios en la Geoquímica de las Fumarolas del Volcán Turrialba, Costa Rica: 1998–2001 (abstract): Colima Volcano: Eighth Internacional Meeting, p. 84.
- Fischer, R.V., and Schmincke, H.-U., 1984, *Pyroclastic rocks*: Berlin, Springer-Verlag, 472 p.
- Gans, P.B., Alvarado, G., Pérez, W., MacMillan, I., and Calvert, A., 2003, Neogene evolution of the Costa Rican Arc and development of the Cordillera Central: Geological Society of America Abstracts with Programs, v. 35, no. 4, p. 74.
- Glazner, A.F., Manley, C.R., Marron, J.S., and Rojstaczer, S., 1999, Fire or ice: Anticorrelation of volcanism and glaciation in California over the past 800,000 years: *Geophysical Research Letters*, v. 26, p. 1759–1762, doi: 10.1029/1999GL900333.
- González-Viquez, C., 1910, Temblores, terremotos, inundaciones, y erupciones volcánicas en Costa Rica 1608–1910: Tipografía de Avelino Alsina, San José de Costa Rica, p. 35–41.
- Hall, K., 1982, Rapid deglaciation as an initiator of volcanic activity: An hypothesis: *Earth Surface Processes and Landforms*, v. 7, p. 45–51.
- Hudnut, K.W., 1983, *Geophysical survey of Irazú Volcano* [Bachelor's thesis]: Dartmouth College, 82 p.
- Krushensky, R.D., and Escalante, G., 1967, Activity of Irazu and Poas Volcanoes, Costa Rica, November 1964–July 1965: *Bulletin of Volcanology*, v. 31, p. 75–84.
- Lachniet, M.S., and Seltzer, G.O., 2002, Late Quaternary glaciation of Costa Rica: *Geological Society of America Bulletin*, v. 114, p. 547–558, doi: 10.1130/0016-7606(2002)114<0547:LQGOCR>2.0.CO;2.
- McGuire, W.J., 1996, Volcano instability: a review of contemporary themes, *in* McGuire, W.J., Jones, A.P., and Neuberg, J., eds., *Volcano instability on the Earth and other planets*: London, Geological Society Special Publication 110, p. 1–23.
- McGuire, W.J., Howarth, R.J., Firth, C.R., Solow, A.R., Pullen, A.D., Saunders, S.J., Stewart, I.S., and Vita-Finzi, C., 1997, Correlation between rate of sea-level change and frequency of explosive volcanism in the Mediterranean: *Nature*, v. 389, p. 473–476, doi: 10.1038/38998.
- Melson, W.G., Barquero, J., Sáenz, R., and Fernández, E., 1985, Erupciones explosivas de importancia en volcanes de Costa Rica: *Costa Rica: Boletín de Vulcanología*, v. 16, p. 15–22.
- Mora, R., Ramírez, C., and Fernández, M., 2004, La actividad de los volcanes de la Cordillera Central, Costa Rica, entre 1998–2002, *in* Soto, G.J. and Alvarado, G.E., eds., *La Vulcanología y su entorno geoambiental*: Revista Geológica de América Central, v. 30, p. 189–197.
- Mullineaux, D.R., and Crandell, D.R., 1981, The eruptive history of Mount St. Helens, *in* Lipman, P.W., and Mullineaux, D.R., eds., *The 1980 eruptions of Mount St. Helens*, Washington: U.S. Geological Survey Professional Paper 1250, p. 3–16.
- Murata, K.J., Dóndoli, C., and Sáenz, R., 1966, The 1963–65 eruption of Irazu Volcano, Costa Rica (the period of March 1963 to October 1963): *Bulletin of Volcanology*, v. 29, p. 765–796.
- Nakada, M., and Yokose, H., 1992, Ice age as a trigger of active Quaternary volcanism and tectonism: *Tectonophysics*, v. 212, p. 321–329, doi: 10.1016/0040-1951(92)90298-K.
- Newhall, C.G., and Self, S., 1982, The volcanic explosivity index (VEI): An estimate of explosive magnitude for historical volcanism: *Journal of Geophysical Research, Oceans and Atmospheres*, v. 87, p. 1231–1238.
- Obando, L.G., and Soto, G.J., 1993, La turbera del Río Silencio (El Cairo, Siquirres, Costa Rica): Paleoaambientes lagunares influenciados por las cenizas del Volcán Turrialba: *Revista Geológica de América Central*, v. 15, p. 41–48.
- Orvis, K.H., and Horn, S.P., 2000, Quaternary glaciers and climate on Cerro Chirripo, Costa Rica: *Quaternary Research*, v. 54, p. 24–37, doi: 10.1006/qres.2000.2142.
- Pyle, D.M., 1989, The thickness, volume and grain size of tephra fall deposits: *Bulletin of Volcanology*, v. 51, p. 1–15, doi: 10.1007/BF01086757.
- Reagan, M.K., 1987, *Turrialba Volcano, Costa Rica: Magmatism at the south-east terminus of the Central American arc* [Ph.D. dissertation]: Santa Cruz, University of California, 216 p.
- Reagan, M.K., and Gill, J.B., 1989, Coexisting calcalkaline and high-niobium basalts from Turrialba volcano, Costa Rica: Implications for residual titanates in arc magma sources: *Journal of Geophysical Research*, v. B94, p. 4619–4633.
- Reagan, M.K., Gill, J.B., Malavassi, E., and García, M.O., 1987, Changes in lava composition at Arenal Volcano, Costa Rica, 1968–85: Realtime monitoring of open-system differentiation: *Bulletin of Volcanology*, v. 49, p. 415–434.
- Reid, M.E., Sisson, T.W., and Brien, D.L., 2001, Volcano collapse promoted by hydrothermal alteration and edifice shape, Mount Rainier, Washington: *Geology*, v. 29, p. 779–782, doi: 10.1130/0091-7613(2001)029<0779:VCPBHA>2.0.CO;2.
- Sáenz, R., Barquero, J., and Malavassi, E., 1982, Excursión al volcán Irazú, USA-CR joint seminar in volcanology: *Boletín de Vulcanología*, v. 14, p. 101–116.
- Siebert, L., 1984, Large volcanic debris avalanches: Characteristics of source areas, deposits, and associated eruptions: *Journal of Volcanology and Geothermal Research*, v. 22, p. 163–197, doi: 10.1016/0377-0273(84)90002-7.
- Siebert, L., Glicken, H., and Ui, T., 1987, Volcanic hazards from Bezymianny and Bandai-type eruptions: *Bulletin of Volcanology*, v. 49, p. 435–459, doi: 10.1007/BF01046635.
- Simkin, T., and Siebert, L., 2002, *Global Volcanism FAQs*: Smithsonian Institution, Global Volcanism Program Digital Information Series, GVP-5, <http://volcano.si.edu/gvp.faq>.
- Soto, G., 1988, Estructuras volcano-tectónicas del Volcán Turrialba, Costa Rica, América Central, *in* Actas Quinto Congreso Geológico Chileno, Santiago, 8–12 de agosto de 1988: Tomo III, p. I-163–I-175.
- Stuiver, M., Reimer, P.J., Bard, E., Beck, J.W., Burr, G.S., Hughen, K.A., Kromer, B., McCormac, G., van der Plicht, J., and Spurk, M., 1998, INTCAL98 radiocarbon age calibration, 24,000–0 cal BP: *Radiocarbon*, v. 40, p. 1041–1083.
- Tournon, J., 1984, *Magmatismes du Mésozoïque à l'actuel en Amérique Centrale: L'exemple de Costa Rica, des ophiolites aux andésites* [PhD Dissertation]: Paris, Université Pierre and Marie Curie, IIX + 335 p.
- Ui, T., 1983, Volcanic dry avalanche deposits-identification and comparison with non-volcanic debris stream deposits, *in* Aramaki, S., and Kushiro, I., eds., *Arc Volcanism: Journal of Volcanology and Geothermal Research*, v. 18, p. 135–150.
- von Seebach, K., 1865, Besteigung des Vulkans Turrialba in Costa Rica: *Petermann's Mitteil*, v. 9, p. 321–324.

TABLE A1. MAJOR AND TRACE ELEMENT DATA FOR TURRIALBA'S LAVAS AND TEPHRAS

Sample Unit	T-1 1 cinder	T-24-2 1 lava	T-37-1 1 cinder	T-37-5 1 cinder	T-51-3 1 cinder	T-51-5 1 cinder	T-131 1 cinder	T-85 1 clike	T-86 1 clike	T-62 2 lava	T-51-1 2 cinder	T-55-i 2 cinder	T-102 2 lava	T-38-5 3 pumice	T-38-5b 3 pumice	T-59 3 cinder
SiO ₂	52.51	52.55	52.64	52.31	52.39	52.13	52.37	51.73	51.96	56.55	54.87	55.21	57.58	61.71	57.34	54.71
TiO ₂	1.04	1.04	1.04	1.39	1.05	1.05	1.05	1.91	1.06	0.91	0.91	0.92	0.77	0.74	1.13	1.44
Al ₂ O ₃	17.18	17.19	17.02	16.82	17.62	17.9	17.14	15.91	17.61	16.66	18.1	17.08	17.58	17.16	15.98	15.63
Fe ₂ O ₃	8.52	8.33	8.48	8.78	8.5	8.43	8.62	9.69	8.53	7.25	7.78	7.46	6.87	5.24	6.84	7.85
MnO	0.14	0.14	0.14	0.14	0.14	0.14	0.14	0.14	0.14	0.12	0.12	0.12	0.12	0.1	0.12	0.12
MgO	6.24	6.24	6.41	5.96	6.04	6.26	6.16	6.48	6.1	5.32	5	5.55	4.02	2.84	5.05	6.19
CaO	9.23	9.19	9.27	9.44	9.15	9.18	9.48	8.93	9.57	7.5	8.16	8.28	7.42	5.06	6.63	7.67
Na ₂ O	3.37	3.47	3.19	3.2	3.26	3.14	3.29	3.6	3.3	3.59	3.22	3.48	3.31	3.92	3.83	3.39
K ₂ O	1.42	1.47	1.45	1.46	1.46	1.4	1.37	1.09	1.37	1.78	1.52	1.59	2.08	2.94	2.56	2.37
P ₂ O ₅	0.37	0.4	0.38	0.52	0.4	0.38	0.39	0.53	0.38	0.32	0.32	0.31	0.26	0.3	0.52	0.63
LOI	-0.02	0.12	-0.01	0.67	-0.05	-0.05	-0.24	-0.17	0.12	0.77	1	-0.01	0.2	0.98	0.2	1.76
total*	100.78	100.67	100.33	100.35	100.1	99.45	99.74	100.34	99.35	99.95	100.7	100.85	99.26	100.22	99.31	100.1
Ni	54.2	58	59.2	58.3	49.9	50.3	51.5	101.5	53	73.7	44.6	54.4	35.7	33	84.9	111.4
Sc	26.1	26.4	27.1	26.5	27	27.5	27.6	21.6	27.7	19.7	23.2	22.5	18.1	10.9	16.1	18.5
Cr	126	142	144	127	125	124	130	186	135	144	86	116	40	54	151	222
Ce	67	67	69	87	68	65	65	82	64	69	56	62	62	87	105	123
Nd	33.8	30.3	34.6	39.9	34.1	32.7	32.7	38.1	31.8	30.9	27.1	29.1	28.3	34	43.8	53
V	232	228	241	233	239	244	243	218	240	187	221	200	157	96	146	184
Ba	674	670	691	680	679	657	662	524	661	798	706	716	845	1059	964	858
La	35.9	33.3	37.8	46.9	37.9	36.4	35.1	42	37.3	38.8	30.6	31.6	32.3	46.7	57.9	68.4
Nb	14	13.1	14	25.4	13.9	13.2	14.2	35.8	13.9	19.5	12	8.9	11.1	18.5	26.5	33.1
Zr	142	142	148	175	143	139	144	194	145	169	132	146	157	245	249	248
Y	22	21.8	21.6	23.3	22.2	20.3	22	25.6	21.6	18.1	17.7	18.3	16.2	22.4	23.1	25.1
Sr	784	802	799	976	773	825	784	887	792	776	832	854	1010	744	883	999
Rb	29.2	28.7	29.3	29.9	29.2	30.8	29.6	22.2	29.3	38.4	31.5	33.9	44.5	74.4	62.5	53
Th	-	5.4	-	5.9	-	-	-	5.5	-	-	-	-	-	13.7	13	12.4
U	-	1.8	-	2	-	-	-	1.6	-	-	-	-	-	4.7	4.1	3.7

Continued

TABLE A1. MAJOR AND TRACE ELEMENT DATA FOR TURRIALBA'S LAVAS AND TEPHRAS (continued)

Sample Unit	T-101-1 3 cinder	T-101-2 3 cinder	T-3 4 pumice	T-4 4 clast	T-35-1 4 pumice	T-35-2 4 cinder	T-35-4 4 clast	T-35-5 4 pumice	T-103-1-3 4 pumice	T-103-6 5 cinder	T-103-7a 7 cinder	T-63 8b lava	T-129 8b lava	T-124 8c lava	T-126 8c lava
SiO ₂	59.61	58.21	58.26	57.59	58.49	58.16	58.21	58.95	58.41	55.97	56.12	62.58	64.09	57.23	57.21
TiO ₂	1.24	1.1	0.89	0.92	0.9	0.92	0.91	0.86	0.92	0.85	0.87	0.67	0.63	0.86	0.83
Al ₂ O ₃	19.5	16.98	17.3	16.88	16.93	16.89	16.87	16.86	16.78	17.18	17.07	16.76	16.53	17.16	17.42
Fe ₂ O ₃	4.8	6.51	6.45	6.62	6.57	6.66	6.62	6.29	6.64	7.79	8.04	5.00	4.62	6.97	6.97
MnO	0.08	0.11	0.12	0.12	0.14	0.12	0.12	0.12	0.12	0.13	0.13	-	0.09	0.12	0.12
MgO	3.63	4.4	3.91	4.08	3.96	4.09	3.94	3.82	3.86	5.03	5.02	3.02	2.22	4.29	4.06
CaO	6.1	7.51	6.66	7.02	6.56	6.69	6.92	6.5	6.68	8.39	8.17	5.05	4.64	7.26	7.49
Na ₂ O	2.66	2.66	3.75	4.15	3.75	3.8	3.7	3.85	3.9	2.66	2.63	3.92	3.88	3.74	3.53
K ₂ O	1.96	2.08	2.31	2.29	2.36	2.34	2.37	2.43	2.37	1.71	1.67	2.77	3.09	2.06	2.08
P ₂ O ₅	0.43	0.45	0.35	0.34	0.34	0.34	0.35	0.33	0.33	0.3	0.29	0.24	0.23	0.31	0.3
LOI	7.29	2.74	1	0.26	0.33	0.26	0.11	0.2	0.12	2.09	3.18	1.37	0.26	-0.05	0.27
total*	100.8	100.94	100.9	99.83	100.33	100.33	99.83	100.07	100.01	100.9	100.84	100.24	100.5	99.74	99.71
Ni	47.8	67.2	27.8	29.4	27.4	28.1	29	28.4	26.3	53.9	65.8	-	16	32.1	32.3
Sc	22.3	19.5	16.8	17.9	16	17.8	17.5	16.9	16.9	25.2	23.4	-	10.6	17.5	19.5
Cr	240	179	55	58	60	61	61	58	59	205	191	-	21	58	50
Ce	98	97	84	83	80	84	85	81	83	73	78	-	85	77	71
Nd	44.7	45	36.8	36.4	33.5	36.6	36.9	35.1	36.2	37.9	41.8	-	33.6	34.7	32.3
V	328	217	155	162	158	161	158	156	158	209	201	-	77	156	159
Ba	774	810	947	936	925	949	955	955	941	740	746	-	1117	913	881
La	50.4	49.8	46.8	46.1	41.9	46.5	44.6	44.1	44.9	39.8	41.9	-	43.8	38.7	38.6
Nb	23.8	21.9	22.3	21.3	21.2	21.9	21.3	21.1	21.5	14.2	14.1	-	19.7	11.5	13.9
Zr	202	197	215	204	208	215	213	217	212	167	167	-	250	179	171
Y	28.2	32.8	22.2	22.4	21.8	22.8	23	22.7	22.6	30	32	-	20.3	20.4	18.9
Sr	895	856	759	798	752	781	774	730	748	645	645	-	710	892	946
Rb	48.6	48.8	55.4	54.8	55.3	58.2	57.8	58	57.8	40.6	38.5	-	78.4	47	47.2
Th	-	-	-	-	10.3	-	-	-	-	-	-	-	-	-	-
U	-	-	-	-	3.5	-	-	-	-	-	-	-	-	-	-

Continued

TABLE A1. MAJOR AND TRACE ELEMENT DATA FOR TURRIALBA'S LAVAS AND TEPHRAS (continued)

Sample Unit	T-65	T-64	T-5	T-22-9	T-69-d	T-70-6	T-70-7	T-70-12	T-70-13	T-76	T-89	T-90	T-7	T-132	C-3
Type	8c lava	8c lava	9 lava	9 lava	9 lava	10 lava	10 lava	11 lava	11 lava	11 cinder					
SiO ₂	57.19	57.49	58.03	58.27	57.81	56.95	57.1	57.92	57.4	57.52	54.97	54.31	56.94	57.74	56.43
TiO ₂	0.79	0.79	0.71	0.71	0.73	0.77	0.76	0.7	0.74	0.71	0.91	0.9	0.86	0.72	1.08
Al ₂ O ₃	17.75	17.85	17.98	18.11	18.15	18.07	18.22	18.03	18.02	18.11	18.46	18.51	17.61	18.07	18.73
Fe ₂ O ₃	6.87	6.92	6.64	6.71	6.65	6.9	6.95	6.82	6.74	6.76	7.81	8.18	6.86	6.57	7.82
MnO	0.12	0.12	0.11	0.11	0.11	0.11	0.12	0.12	0.11	0.11	0.13	0.12	0.11	0.1	0.11
MgO	4.17	3.96	3.77	3.79	3.68	4.04	4.23	3.8	4.13	3.85	4.61	4.44	4.55	4.13	4.62
CaO	7.4	7.05	7.12	7.01	7.36	7.58	7.16	7.13	7.2	7.36	8.37	8.57	7.35	7.43	6.8
Na ₂ O	3.3	3.39	3.76	3.52	3.55	3.74	3.63	3.66	3.65	3.71	3.3	3.38	4	3.85	2.44
K ₂ O	2.13	2.15	1.63	1.51	1.68	1.55	1.53	1.57	1.75	1.6	1.11	1.26	1.41	1.11	1.65
P ₂ O ₅	0.28	0.29	0.26	0.27	0.29	0.3	0.3	0.26	0.27	0.28	0.33	0.34	0.31	0.28	0.32
LOI	1.06	0.69	0.34	0.35	0.55	0.35	0.41	0.59	0.48	0.52	1.32	1.76	0.7	0.81	3.92
total*	99.63	100.65	101.21	99.86	99.72	100.32	100.3	100.79	100.74	99.51	99.46	99.6	99.92	100.19	101
Ni	37.9	34.4	24.5	23.5	24.7	28.6	28.6	23.9	25.8	24.5	30.1	29.2	49.8	44.1	22.7
Sc	18.5	17.5	17.4	15.9	16.5	18.4	17.3	16.4	16.9	16.4	25.4	23.1	18.6	16.7	23.9
Cr	40	44	16	11	16	29	21	10	18	10	51	46	56	60	79
Ce	54	64	35	35	35	40	41	35	35	36	58	52	52	43	58
Nd	26.5	28.4	17.8	17.7	17.9	21.9	22.6	18.4	18.7	20	27.9	25.9	24.1	20.7	28.1
V	160	149	152	138	148	167	174	142	155	148	210	216	179	156	247
Ba	819	859	713	699	716	700	702	722	711	718	689	693	794	694	684
La	30.3	35.4	17.5	15	15.7	18.4	17.6	18	14.7	13.9	25.6	28.6	26.1	17.6	31.5
Nb	10.3	11.9	6.2	7.2	6.4	6.4	6.6	6.1	6.3	6.4	9.5	9.3	9.5	7	11.7
Zr	156	168	98	99	96	91	93	96	95	94	109	111	117	93	142
Y	16.9	17.1	13.1	13.7	14.5	16.1	16	13.5	13.7	12.8	17.3	18.2	15.4	10.9	22.7
Sr	987	978	1069	1088	1070	1087	1090	1095	1062	1083	886	883	933	999	761
Rb	43.9	46.8	29.8	27.4	29.9	27	27.2	28.9	28.8	28.4	21.5	24.1	27.4	20.4	36.6
Th	-	9.3	-	-	-	-	-	3	-	-	-	-	3.3	-	-
U	-	2.8	-	-	-	-	-	1.4	-	-	-	-	1.3	-	-

Continued

TABLE A1. MAJOR AND TRACE ELEMENT DATA FOR TURRIALBA'S LAVAS AND TEPHRAS (continued)

Sample	T-68	T-67	T-2	T-66	T-69-g	T-70-2	C-8	T-10	T-57	T-11	T-47	T-81	T-91	T-108-1	T-108-2
Unit	12	13	14	14	14	14	15	15	15	15	15	15	15	15	15
Type	lava	lava	lava	lava	lava	lava	lava	clast	lava	lava	lava	lava	lava	lava	lava
SiO ₂	64.11	55.18	59.47	59.46	59.53	58.75	63.28	51.95	59.12	56.24	64.87	53.37	51.18	51.54	52.73
TiO ₂	0.6	0.87	0.74	0.74	0.74	0.76	0.57	1.13	0.76	0.98	0.67	1	1.15	1.14	0.95
Al ₂ O ₃	16.65	16.93	17.19	17.77	17.54	17.46	16.04	18.19	17.04	17.53	15.76	17.61	17.63	17.73	18.38
Fe ₂ O ₃	4.81	7.99	6.29	6.26	6.34	6.6	4.78	9.12	6.94	7.34	4.42	7.8	8.51	8.54	8.06
MnO	0.09	0.13	0.11	0.1	0.1	0.09	0.09	0.15	0.11	0.13	0.08	0.13	0.15	0.14	0.13
MgO	1.93	6.07	3.99	3.52	3.67	3.99	3.47	5.53	3.91	4.37	2.45	5.5	6.32	6.03	5.21
CaO	4.51	8.32	6.27	6.32	5.94	6.62	4.7	9.23	5.94	6.73	4.06	8.97	9.5	9.71	9.48
Na ₂ O	3.88	2.76	3.53	3.33	3.62	3.49	3.78	3.06	3.39	4.09	4.05	3.76	3.79	3.57	3.55
K ₂ O	3.11	1.42	2.13	2.19	2.21	1.93	3.09	1.33	2.48	2.17	3.41	1.48	1.34	1.21	1.19
P ₂ O ₅	0.33	0.34	0.28	0.31	0.31	0.31	0.2	0.32	0.31	0.42	0.25	0.39	0.43	0.41	0.33
LOI	1.06	1.62	2.09	1.48	1.28	2.56	0.37	0.2	1.31	1.05	0.3	0.87	0.12	0.34	0.49
total*	100.44	100.01	100.78	99.81	99.85	99.81	100.36	99.63	99.95	99.36	99.67	99.92	101.38	100.17	100.35
Ni	12.4	78.8	47.6	48.9	46.9	61.9	51.8	39.2	63.4	44.2	23.7	51.9	36.9	40.8	28.7
Sc	9.6	24.1	17	16.7	15.8	18.4	10.8	26.9	18.5	17.1	9.6	23.4	26.5	27.5	25.6
Cr	12	206	77	55	77	103	137	51	129	79	42	93	96	100	63
Ce	98	65	68	66	71	66	71	40	89	95	99	70	72	70	49
Nd	39.4	32.6	30.4	28.7	30.1	30.6	30.5	23.6	42.8	42.6	40.1	35.2	32.1	36.4	25
V	84	213	161	163	151	158	92	269	164	176	87	251	251	265	232
Ba	1191	685	977	923	918	875	1027	542	928	1014	1218	741	643	668	665
La	56.8	36.6	36.9	37.5	36.4	37.8	38.9	23	49.3	57.4	55.4	40.7	37.7	41.4	26.6
Nb	23.2	13.2	14.9	14.5	15.4	13.5	18.8	9.5	17.5	20	25.6	12.4	12.4	12.5	9.2
Zr	280	157	166	170	182	165	243	115	212	199	293	132	131	128	110
Y	24.6	30.8	22.4	21.3	20.4	18.8	22.1	23.2	35.5	22.7	27	20.8	22.9	22.4	19.1
Sr	695	633	771	794	745	752	575	944	634	880	565	963	912	898	921
Rb	82.5	25.9	46.6	50.8	50	43.4	80.9	22.8	60	48.8	90	24.9	23.3	22	20.8
Th	—	—	—	—	—	—	—	—	—	—	—	—	—	—	—
U	—	—	—	—	—	—	—	—	—	—	—	—	—	—	—

Note: All major and trace element data except U and Th were collected by XRF techniques described in Reagan et al. (1987). U and Th were analyzed by alpha spectrometry techniques described in Reagan et al. (1989). Sample locations are in Reagan (1987) and can be obtained from the first author.
 *All major elements are normalized to 100% the listed total is before normalization.